Nanomanufacturing
University of Michigan
ME599-002 | Winter 2010

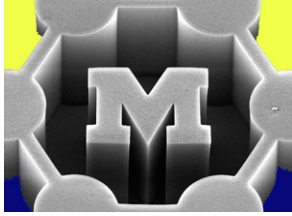

10: **Electrostatics in solution**

February 15, 2010

John Hart
ajohnh@umich.edu
http://www.umich.edu/~ajohnh

Announcements

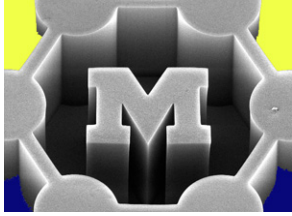

- Video assignment discussion/questions
  - Example: http://vimeo.com/3315489
- PS2 due next Monday (Feb/22)

Recap: small-scale flows

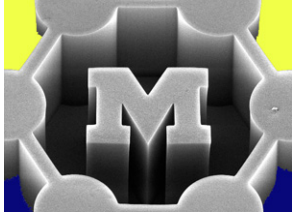

- Wall friction grows nonlinearly as flow scale (e.g., pipe diameter) decreases
- However, when wall friction dominates, we must consider the nature of molecule-wall interactions, called **slip**
- We define flow regimes by Knudsen number,

$\mathrm{Kn} = \lambda / L_o$ Gases, l = mean free path

$\mathrm{Kn} = b / L_o$ Liquids, b = slip length

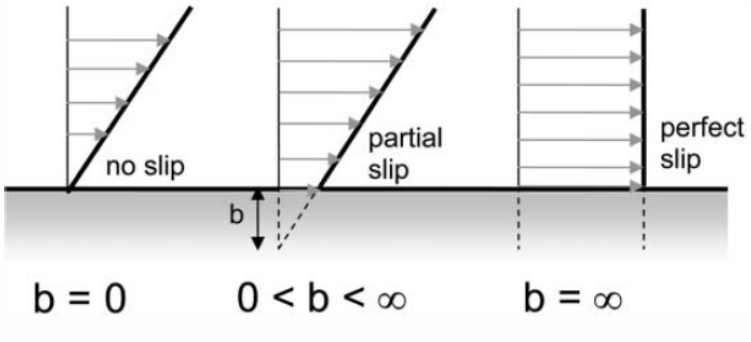

$$Q_{i,s} = -\pi \frac{dp}{dz}\left(\frac{R^4}{8\mu} + \frac{sR^3}{2\mu}\right)$$

- We can superimpose slip upon a no-slip model

What's the molecular origin of slip?

- Fluid-fluid interactions are stronger than fluid-wall interactions (e.g., hydrophobicity).
- Surface roughness traps gas molecules dissolved in the liquid, creating a lubrication layer at the wall. Here, what happens at high Re?
- Molecules "hop" between minimum-energy sites in the wall lattice; therefore slip is a rate process and slip length depends on temperature.

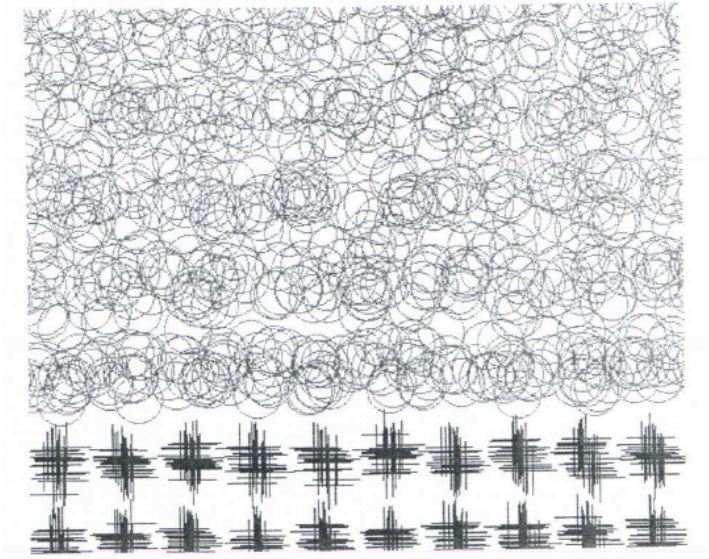

Squires and Quate, Rev Mod Phys 77:977, 2005.
Lichter et al., Phys Rev Lett 98:226001, 2007.

Measuring gas flows in microchannels

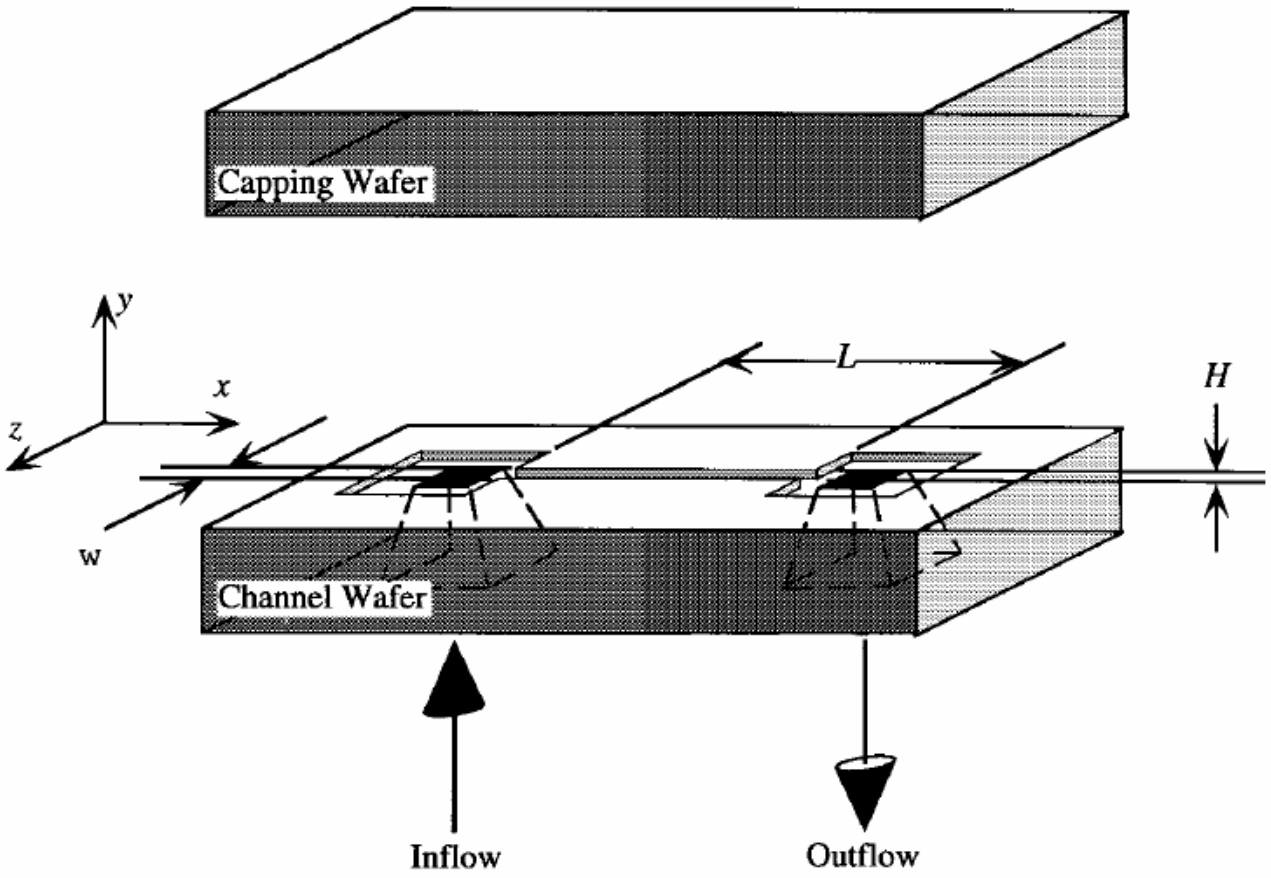

ARACTERIZATION

Parameter	Nominal Value (μm)	Variation (μm)
length (L)	7500	± 10
width (w)	52.25	± 0.25
height (H)	1.33	± 0.01
surface roughness	$\leq 0.65 \times 10^{-3}$	NA

Arkilic et al., J MEMS 6(2):167, 1997.

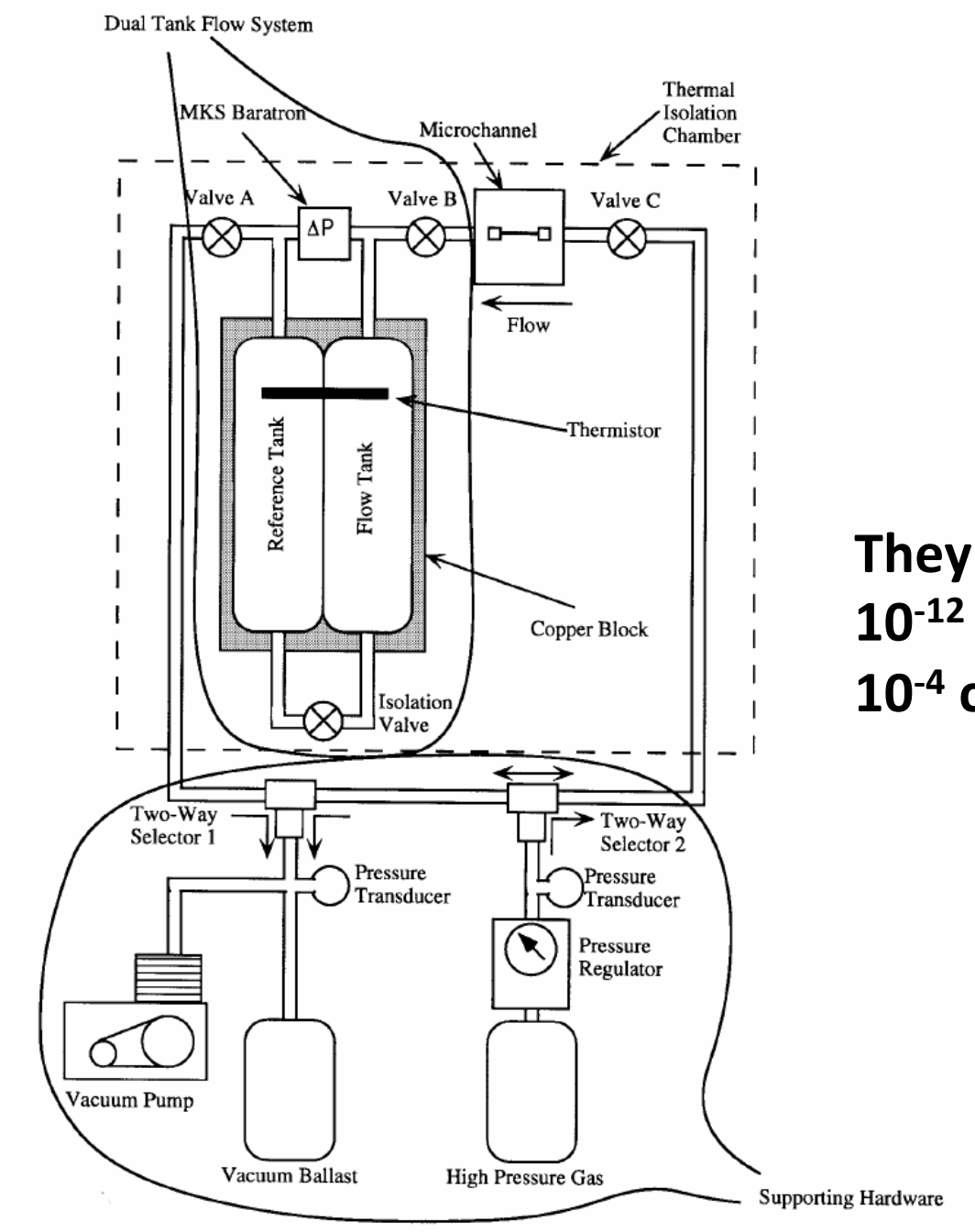

They measured
10^{-12} kg/s
10^{-4} cm^3/s

Arkilic et al., J MEMS 6(2):167, 1997.

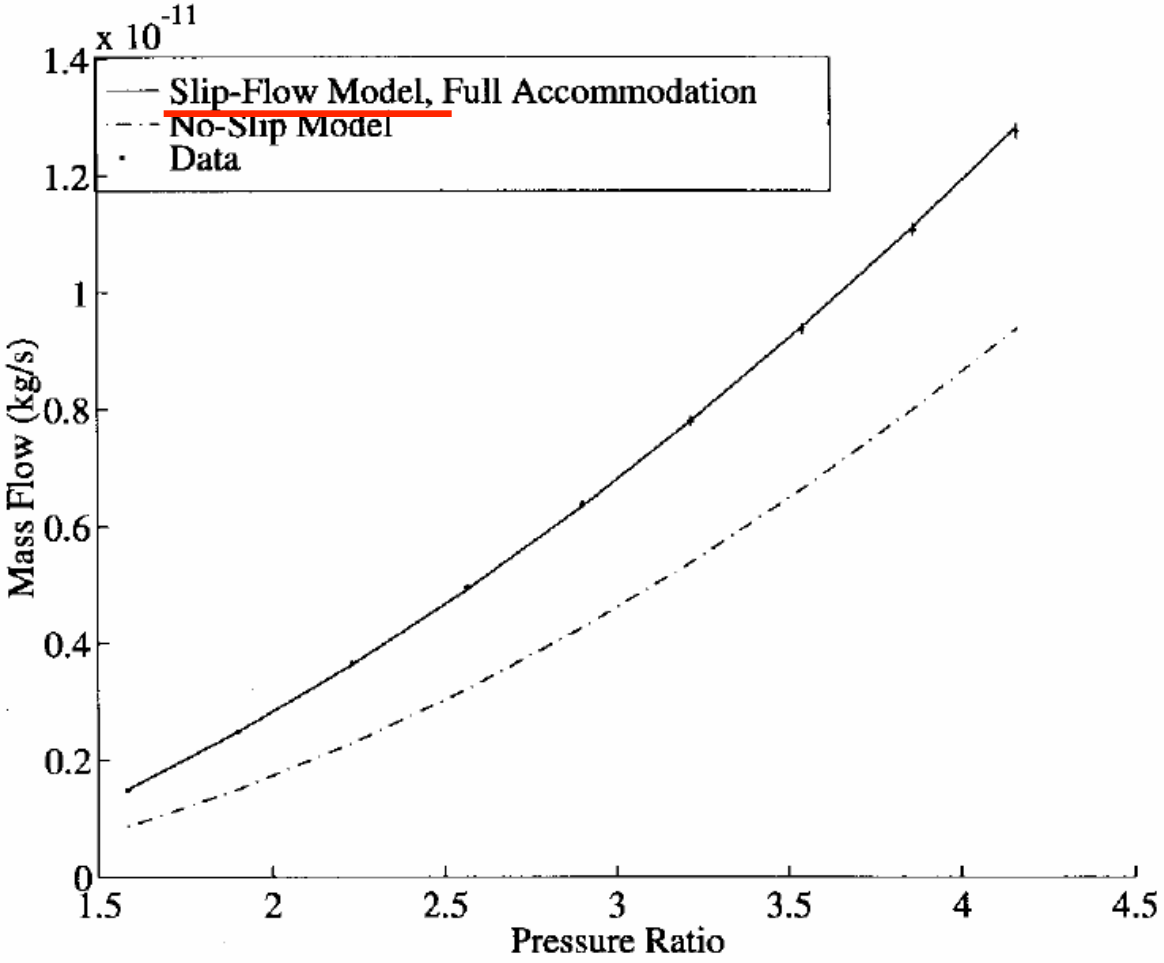

Fig. 10. Helium mass flow for 1.33-μm channel (95% confidence intervals indicated). The solid curve is the solution to (21), assuming full tangential momentum accommodation, and the dashed curve is the solution to (21) setting $K = 0$ (no-slip solution).

Arkilic et al., J MEMS 6(2):167, 1997.

Flow *through* CNTs

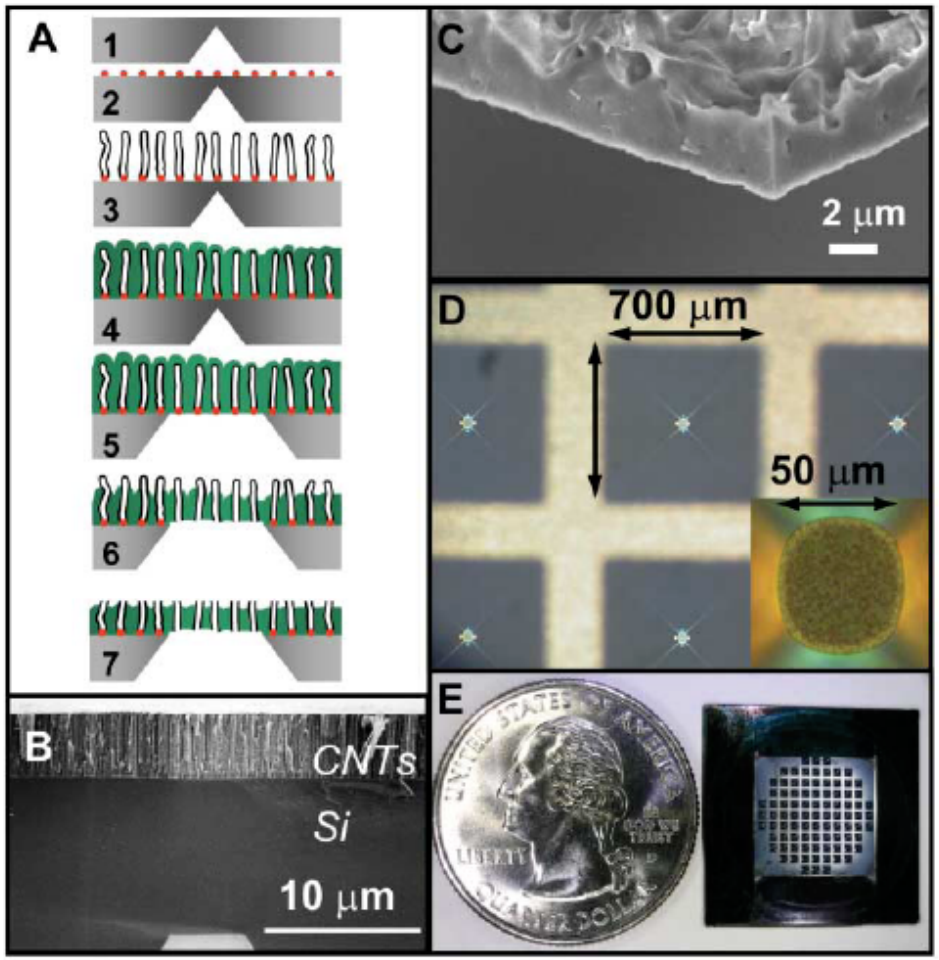

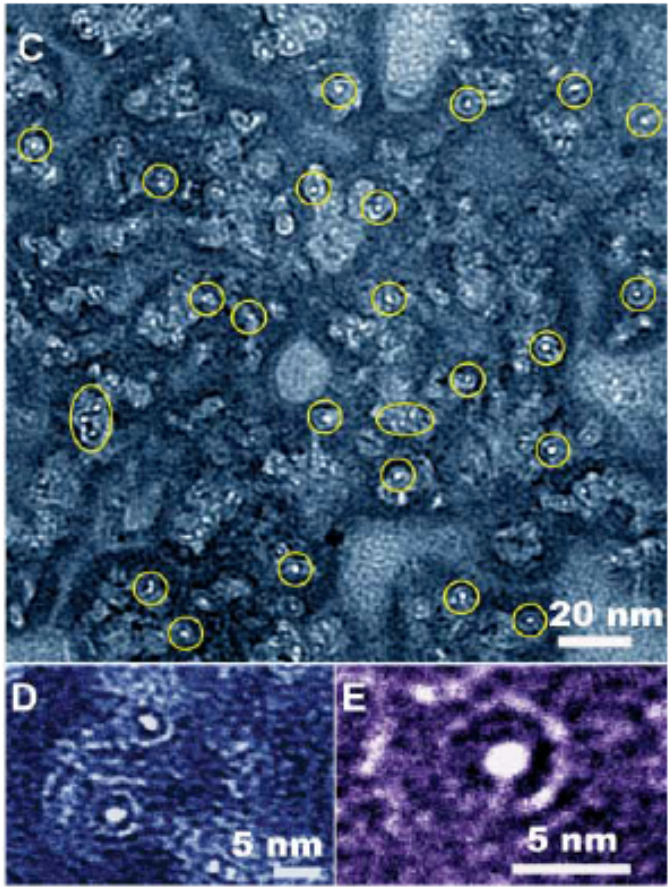

Fig. 1. (**A**) Schematic of the fabrication process. Step 1: microscale pit formation (by KOH etching). Step 2: catalyst deposition/annealing. Step 3: nanotube growth. Step 4: gap filling with low-pressure chemical vapor–deposited Si_3N_4. Step 5: membrane area definition (by XeF_2 isotropic Si etching). Step 6: silicon nitride etch to expose nanotubes and remove catalyst nanoparticles (by Ar ion milling); the membrane is still impermeable at this step. Step 7: nanotube uncapping (reactive ion etching); the membrane begins to exhibit gas permeability at this step. (**B**) SEM cross section of the as-grown DWNTs (CNTs). (**C**) SEM cross section of the membrane, illustrating the excellent gap filling by silicon nitride. (**D**) Photograph of the open membrane areas; inset shows a close-up of one membrane. (**E**) Photograph of the membrane chip that contains 89 open windows; each window is 50 μm in diameter.

Holt et al., Science 312:1034-1037, 2006.

Flow *through* CNTs

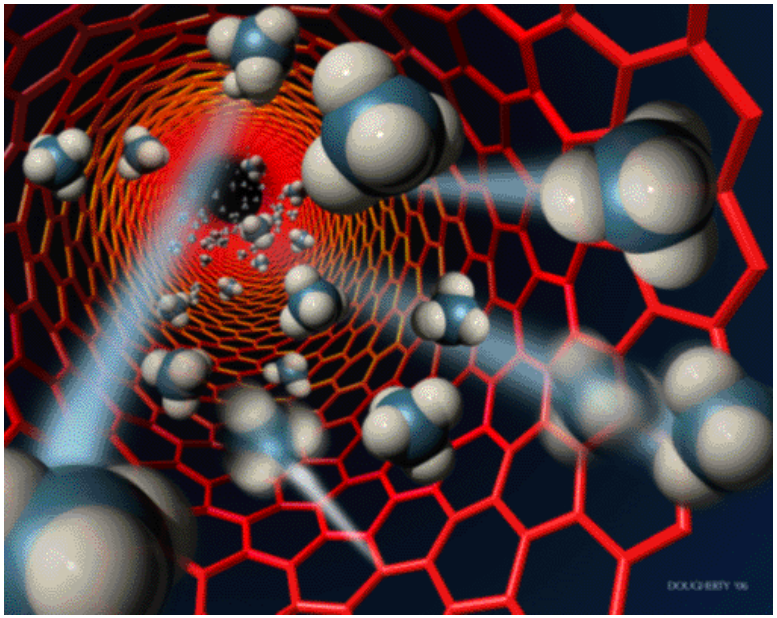

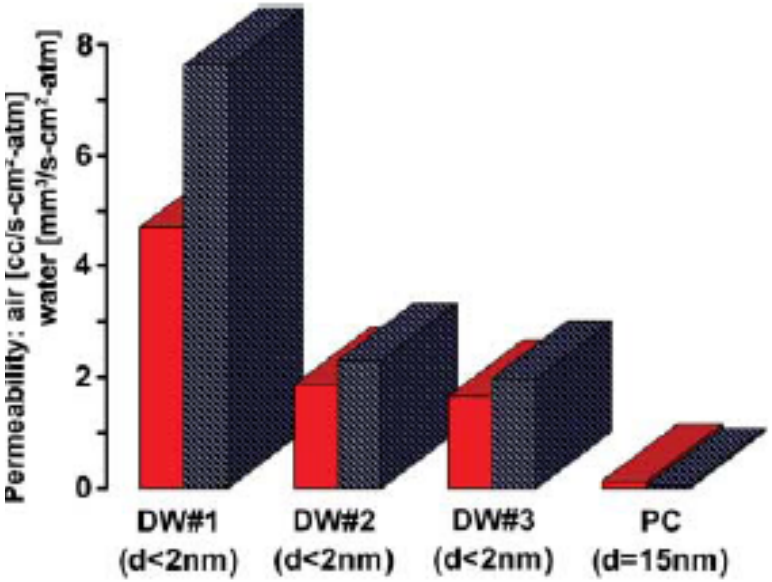

Fig. 4. Air (red) and water (blue) permeability as measured for three DWNT membranes (DW#1, 2, and 3) and a polycarbonate membrane (PC). Despite considerably smaller pore sizes, the permeabilities for all DWNT membranes greatly exceed those of the polycarbonate membrane.

Membrane	Pore diameter (nm)	Pore density (cm^{-2})	Thickness (μm)	Enhancement over Knudsen model* (minimum)	Enhancement over no-slip, hydrodynamic flow† (minimum)	Calculated minimum slip length‡ (nm)
DWNT 1	1.3 to 2.0	$\leq 0.25 \times 10^{12}$	2.0	40 to 120	1500 to 8400	380 to 1400
DWNT 2	1.3 to 2.0	$\leq 0.25 \times 10^{12}$	3.0	20 to 80	680 to 3800	170 to 600
DWNT 3	1.3 to 2.0	$\leq 0.25 \times 10^{12}$	2.8	16 to 60	560 to 3100	140 to 500
Polycarbonate	15	6×10^{8}	6.0	2.1	3.7	5.1

*From (*18*). †From (*26*). ‡From (*29*).

Holt et al., Science 312:1034-1037, 2006.

Extreme slip flow through CNTs

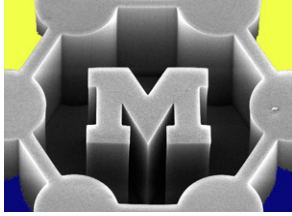

Table 1 | Pressure-driven flow through aligned MWCNT membrane

Liquid	Initial permeability*	Observed flow velocity†	Expected flow velocity†	Slip length (mm)
Water	0.58	25	0.00057	54
	1.01	43.9	0.00057	68
	0.72	9.5	0.00015	39
Ethanol	0.35	4.5	0.00014	28
iso-Propanol	0.088	1.12	0.00077	13
Hexane	0.44	5.6	0.00052	9.5
Decane	0.053	0.67	0.00017	3.4

MWCNT, multiwalled carbon nanotube. For details of methods, see supplementary information. *Units, cm^3 per cm^2 min bar. †Flow velocities in cm s^{-1} at 1 bar. Expected flow velocity is that predicted from conventional flow.

Majumder et al., Nature 438:44, 2005.

Importance of gas damping in MEMS: DMD micromirrors

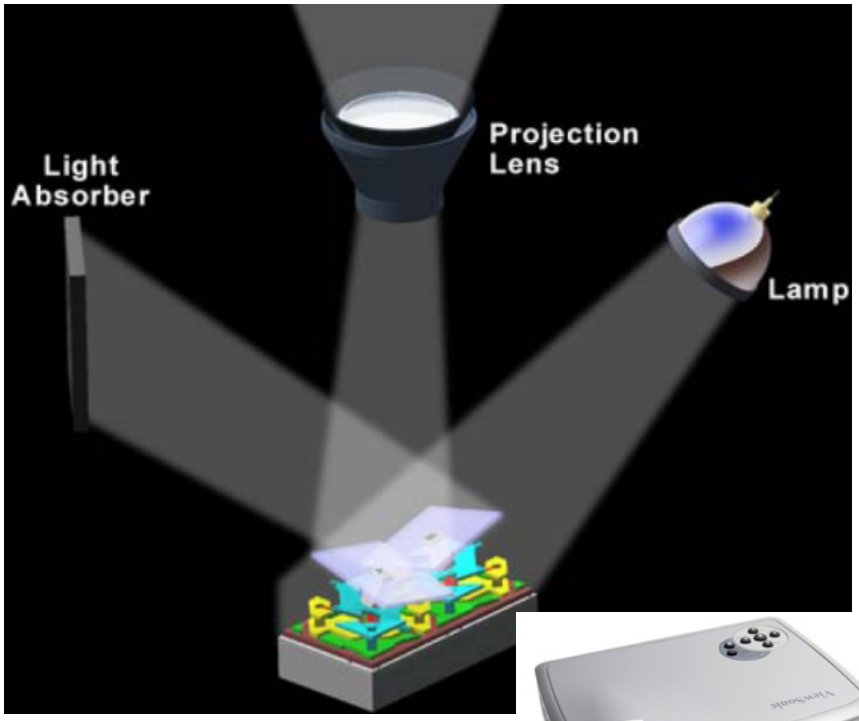

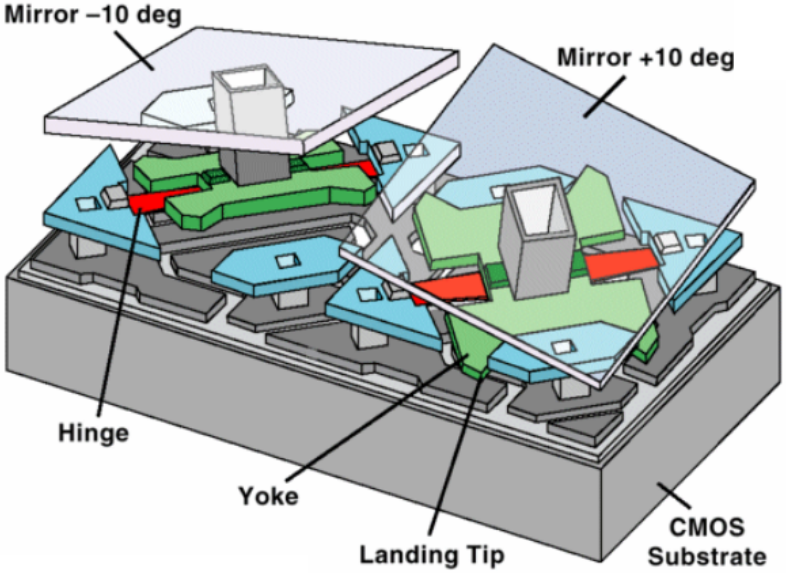

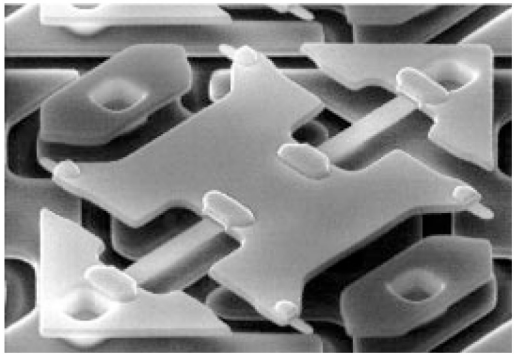

Mirror dynamics at various ambient pressures

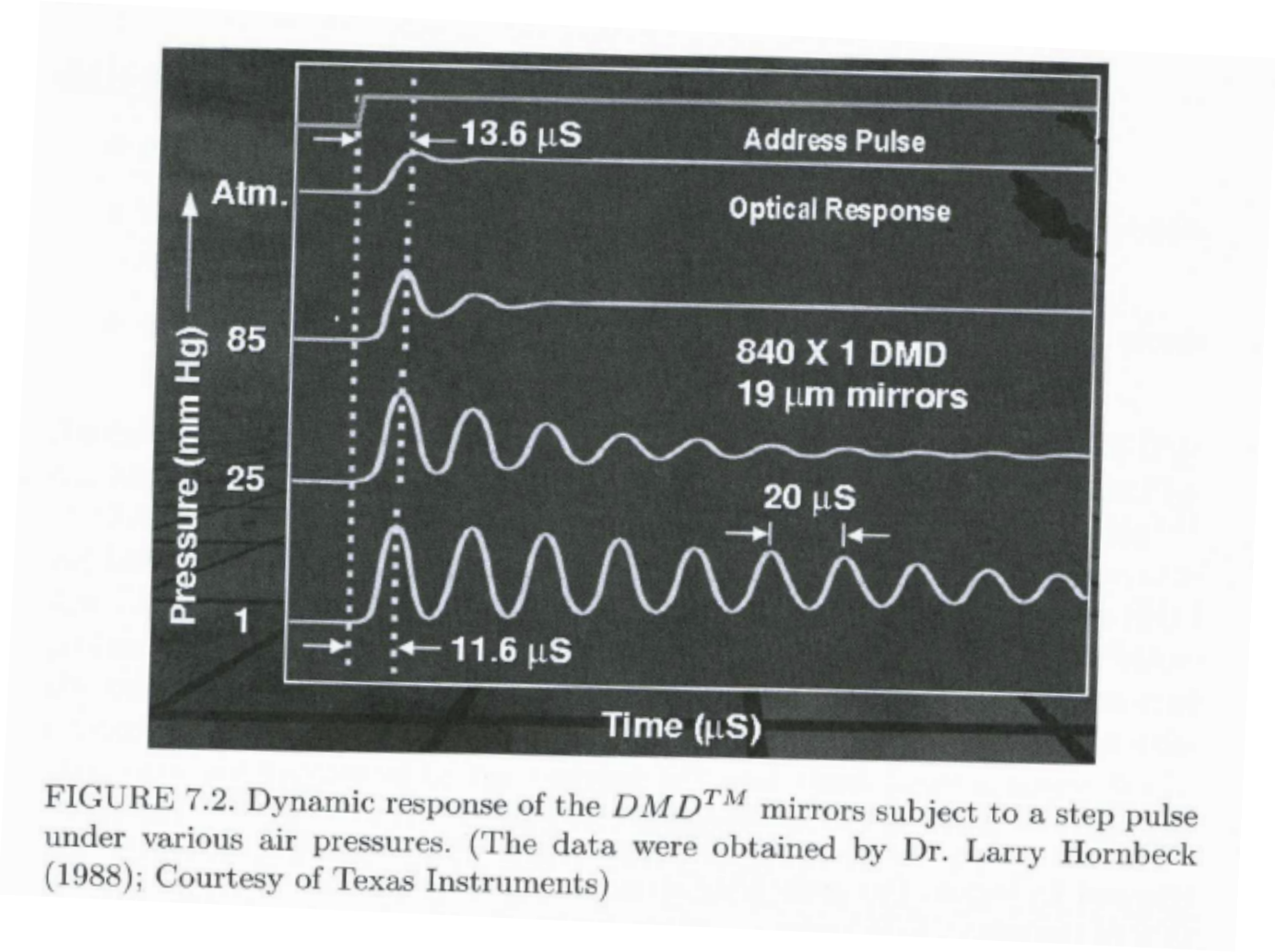

FIGURE 7.2. Dynamic response of the DMD^{TM} mirrors subject to a step pulse under various air pressures. (The data were obtained by Dr. Larry Hornbeck (1988); Courtesy of Texas Instruments)

Karniadakis and Beskok.

Today's agenda

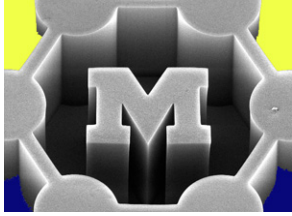

- How surfaces become charged in solution
- Modeling the electrical "double layer"
- Competition between electrostatic repulsion and VDW attraction forces (DLVO theory) → stability vs. coagulation
- Nanofluidic transistors
- Electrophoresis

Today's readings (ctools)

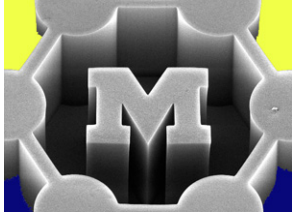

Nominal:

- Hiemenz and Rajagopalan, excerpt on "The electrical double layer and double-layer interactions", from Principles of Colloid and Surface Chemistry
- Karnik et al., "Electrostatic control of ions and molecules in nanofluidic transistors"

Extras:

- Israelachvili, excerpt on "Electrostatic forces between surfaces in liquids", from Intermolecular and Surface Forces

  → same topics as Hiemenz above
- Bouzigues et al., "Nanofluidics in the Debye layer at hydrophilic and hydrophobic surfaces"

  → measurements of slip length on charged surfaces

Surfaces become charged in solution –WHY?

- Ionization or dissociation of surface groups, e.g., -COOH → $-COO^- + H^+$
- Adsorption of ions from solution

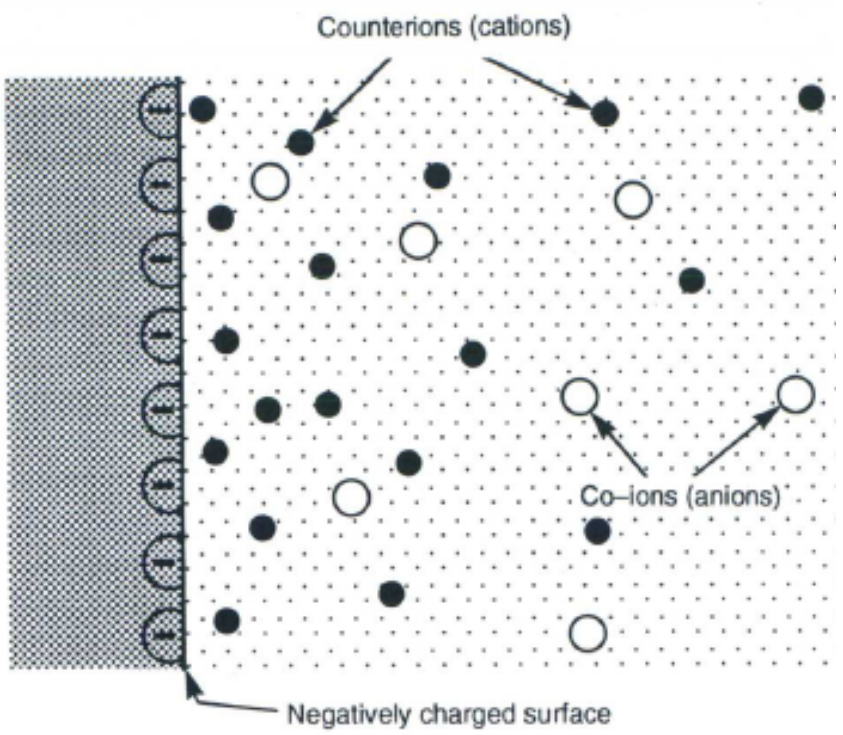

→ Charged surfaces are balanced by counterions in solution, so electrical neutrality is preserved

→ Some counterions adsorb to the surface, and others are distributed near the surface within the **double layer**

→ **This is very important for interactions between nanostructures in solution**

Ion concentration profiles

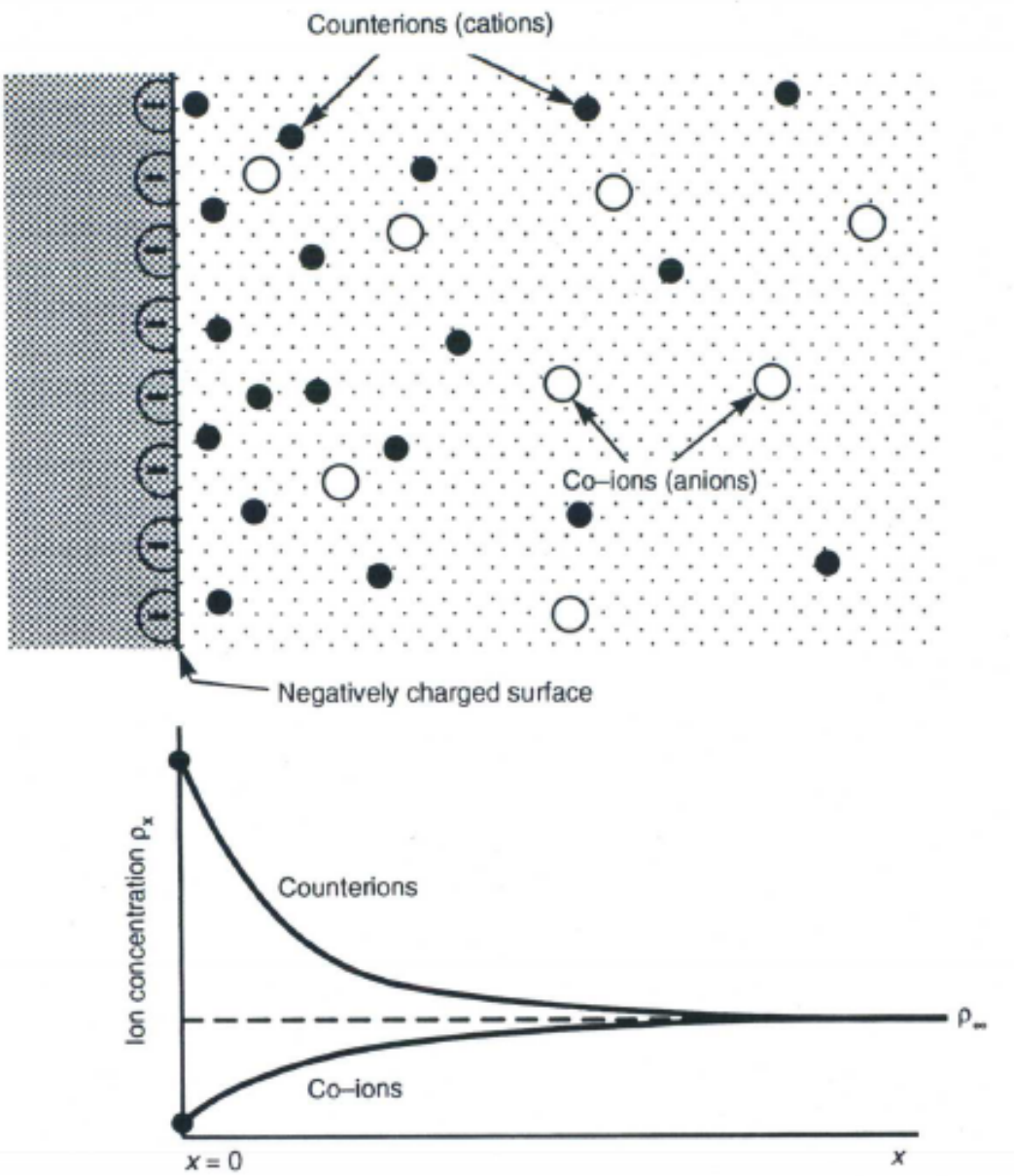

Israelachvili, Mulvaney.

total electrical neutrality

planar, isolated, constant potential

$$\nabla^2 \psi = -\rho^+ / \varepsilon$$

ρ^+: charge density $[C/m^3]$

ε: permittivity

$$\varepsilon = \varepsilon_r \varepsilon_0$$

ε_0: vacuum

$\rho^+(x, y, z)$

$$\frac{d^2\psi}{dx^2} = \frac{-\rho^+(x)}{\varepsilon}$$

ε: constant

BCs: $\psi(0) = \psi_0$, $\psi(\infty) = 0$

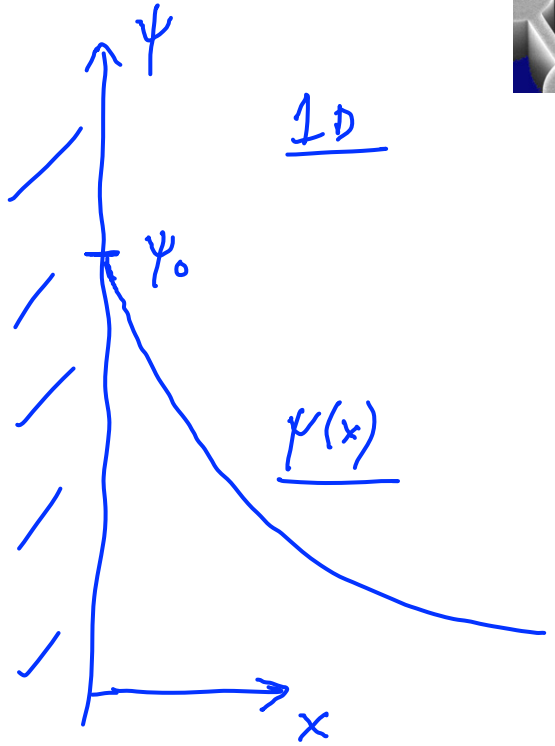

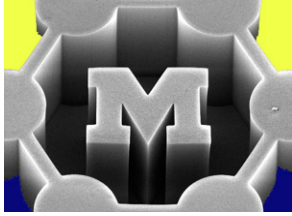

ions in solution obey Boltzmann distribution

$$n_i / n_{i,\infty} = \exp\left\{ \frac{-z_i e \psi}{k_b T} \right\}$$

- n_i: # ions/vol at ψ
- $n_{i,\infty}$: at ∞
- z_i: valence of ion (Na$^+$, $z = 1$; Zn^{2+}, $z = 2$)
- e: charge electron
- $k_b T$: thermal energy

$$\rho^+ = z_i e n_i$$

Na$^+$
Cl$^-$

Multiple ions, add charge densities

$$\rho^+ = \sum z_i e n_i = \sum z_i e n_{i,\infty} \exp\left\{ \frac{-z_i e \psi}{k_b T} \right\}$$

$n_{i,\infty}$: concentration in bulk

Poisson / Boltzmann eqn.

$$\frac{d^2\psi}{dx^2} = \frac{-e}{\varepsilon} \sum_i z_i n_{i,\infty} \exp\left\{ -z_i e\psi / k_b T \right\}$$

$z_i e\psi \ll k_b T$, $\frac{k_b T}{e} @ 298K = 25.7\ mV$

"low surface potential"

$$\frac{d^2\psi}{dx^2} = \left(\left(\frac{e^2}{\varepsilon k_b T} \right) \sum z_i^2 n_{i,\infty} \right) \psi$$

$$\kappa^2 = \left(\frac{e^2}{\varepsilon k_b T} \right) \sum z_i^2 n_{i,\infty} \,, \qquad \frac{d^2\psi}{dx^2} = \kappa^2 \psi$$

κ^{-1} Debye length

"debye layer thickness" [nm]

$-x/(\kappa^{-1})$

$$\psi = \psi_0 e^{-\kappa x} \quad \text{or} \quad \psi = \psi_0 e$$

$\kappa^{-1} = 3.04\ nm.$!

unit conversion.

molarity

$$n_i = 1000\, M_i N_A$$

$$\text{ions}/M^3 = \left(L/M^3\right)\left(\text{Mol}/L\right)\left(\text{ions}/\text{Mol}\right)$$

$$\kappa = \left[\left(\frac{1000\, e^2 N_A}{\epsilon_0 k_b T} \right) \left(\sum z_i^2 M_i \right) \right]^{1/2}$$

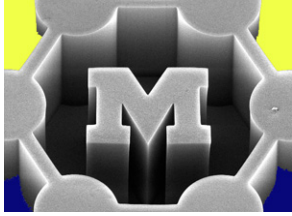

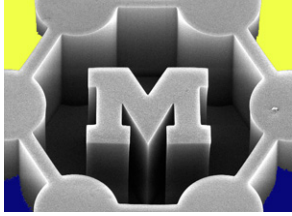

Effect of electrolyte concentration and valence (Debye-Huckel approximation)

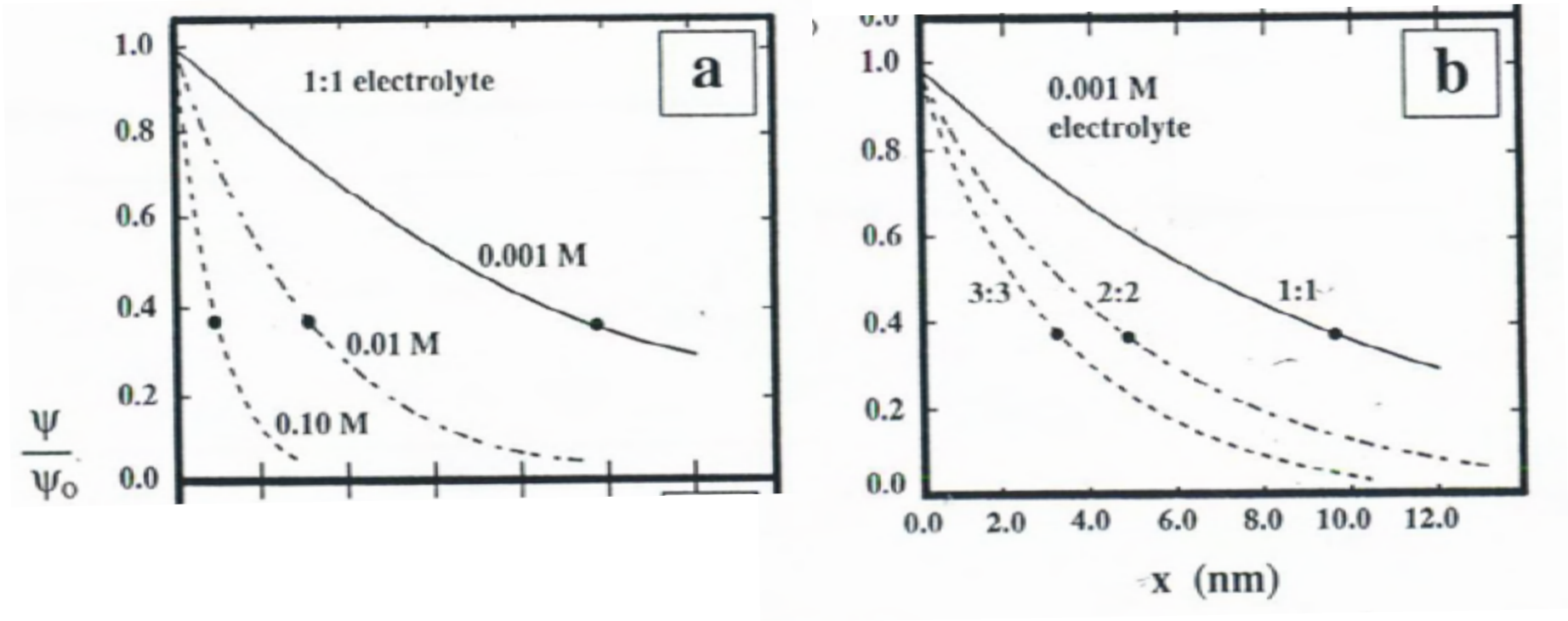

Hiemenz and Rajagopalan.

Comparison of double layer models

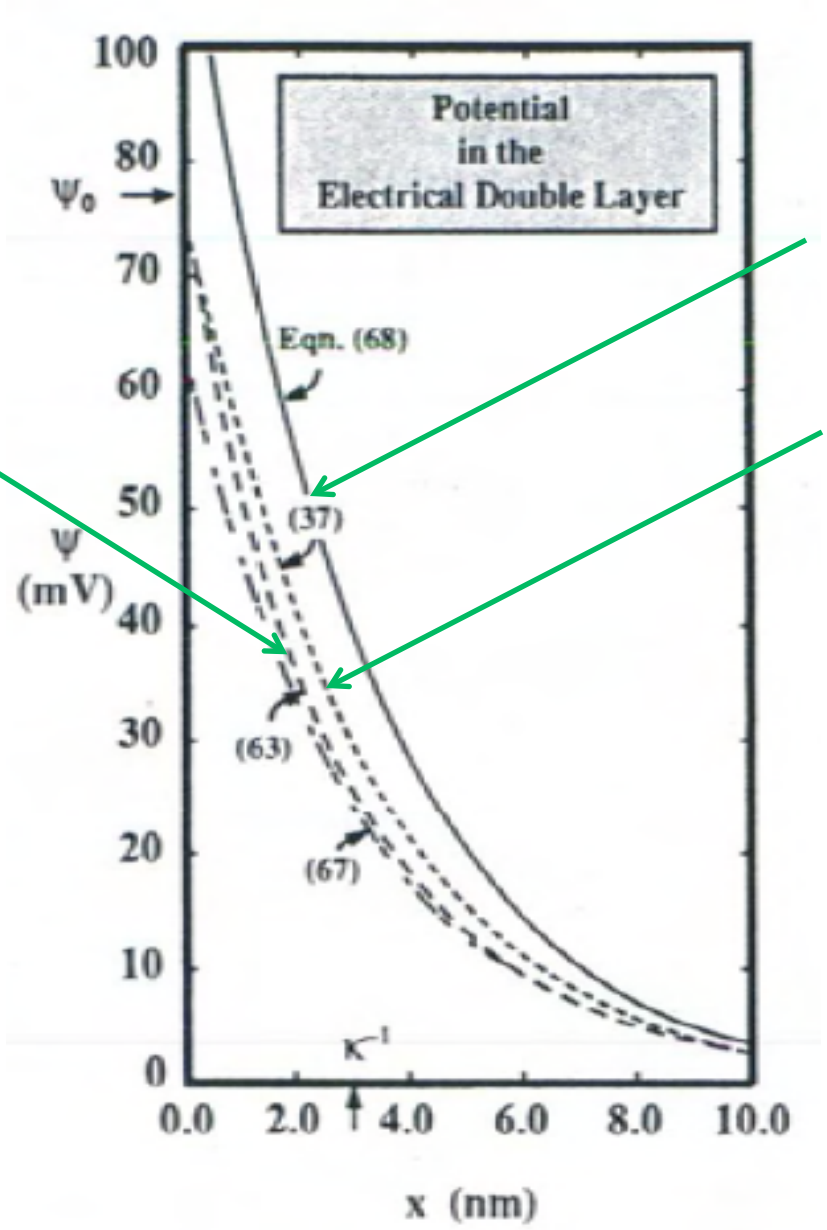

Large Ψ_0

Exact solution (Gouy-Chapman)

Debye-Huckel approximation

0.01M solution of 1:1 electrolyte

Hiemenz and Rajagopalan.

Limiting solutions for small (spherical) and large (locally planar) particles

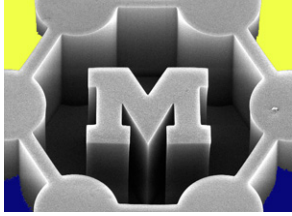

TABLE 5.1 Solutions to the Poisson–Boltzmann equation for microparticles and nanoparticles

	Small κa	Large κa
Low potentials	$\psi(r) = \psi_0 \frac{a}{r} \exp[-\kappa(r-a)]$	$\psi(x) = \psi_0 \exp(-\kappa x)$
High potentials	$\nabla^2\psi = \frac{2zn^\infty e}{\varepsilon_r\varepsilon_0} \sinh\left(\frac{e\psi}{kT}\right)$	$\tanh\left(\frac{ze\psi(x)}{4kT}\right) = \tanh\left(\frac{ze\psi_0}{4kT}\right) \exp(-\kappa x)$
	where $\kappa^2 = \frac{2z^2e^2n^\infty}{\varepsilon_r\varepsilon_0 kT}$	

Hiemenz and Rajagopalan.

Repulsion between overlapping layers

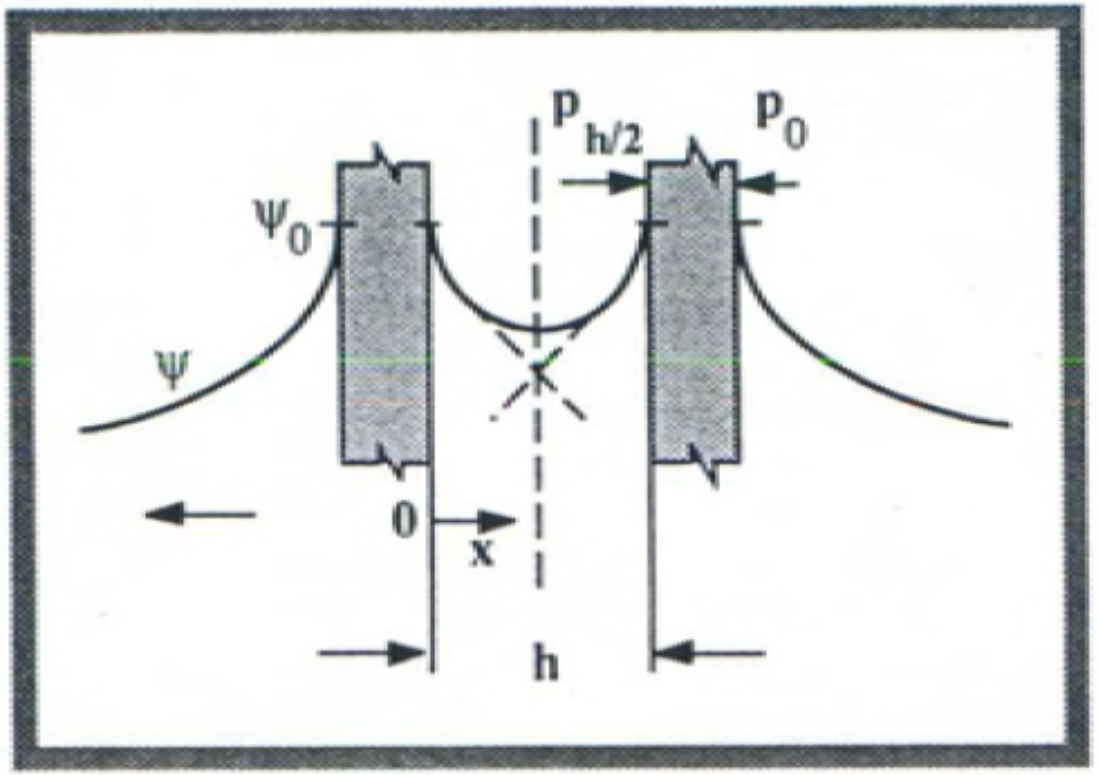

Hiemenz and Rajagopalan.

additive potentials

$h > \lambda$

$\Sigma F = 0$

$F_x = -\frac{dp}{dx}$

$F_{el} = -\rho^* \frac{d\psi}{dx}$

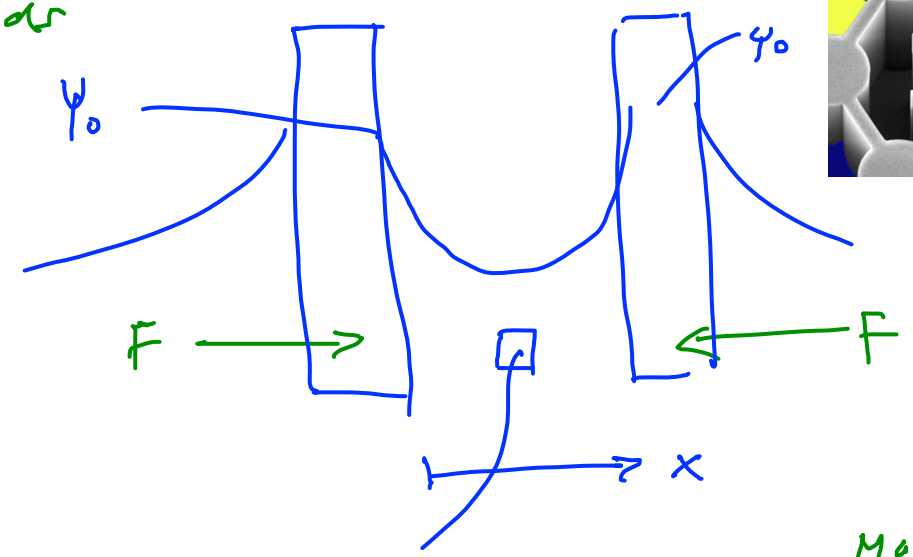

$\Sigma F = 0$

$F_x + F_{el} = 0$

$\frac{dp}{dx} + \rho^* \frac{d\psi}{dx} = 0$

$\rho^* = -\varepsilon \frac{d^2\psi}{dx^2}$

$\frac{dp}{dx} - \varepsilon \left(\frac{d\psi}{dx}\right)\left(\frac{d^2\psi}{dx^2}\right) = 0$

$\frac{1}{2}\frac{d}{dx}\left(\frac{d\psi}{dx}\right)^2$

Maxwell pressure electric field,

$\frac{d}{dx}\left(p - \frac{\varepsilon}{2}\left(\frac{d\psi}{dx}\right)^2\right) = 0$

$= \text{constant}$

$$F_R = 64 k_b T n_\infty \Phi_0^2 \exp(-\kappa h)$$

h: separation

$$\Phi_0 = \left(\frac{\Delta - 1}{\Delta + 1}\right)$$

← Gouy–Chapman solution

$$\Delta = \exp\left(\frac{ze\psi}{2k_b T}\right)$$

← 1:1 electrolyte

$$\kappa^{-1} \propto n_\infty^{-1/2},$$

↑ n_∞

F_R ↓

$$F_R = c_1 n_\infty \exp\left(-c_2 n_\infty^{1/2}\right)$$

← dominate

$$V = \int_0^V dU = \int_\infty^h -F_R(h)\,dh$$

energy of interaction

$$U_{ES}(h) = 64 k_b T \eta_\infty \underline{P}_0^2 \kappa^{-1} \exp(-h\kappa)$$

total interaction energy: $U_{tot} = U_{ES} + U_{VDW}$

"equilibrium": $\left.\frac{dU_{tot}}{dD}\right|_h = 0$

Stabilization of colloids: DLVO theory

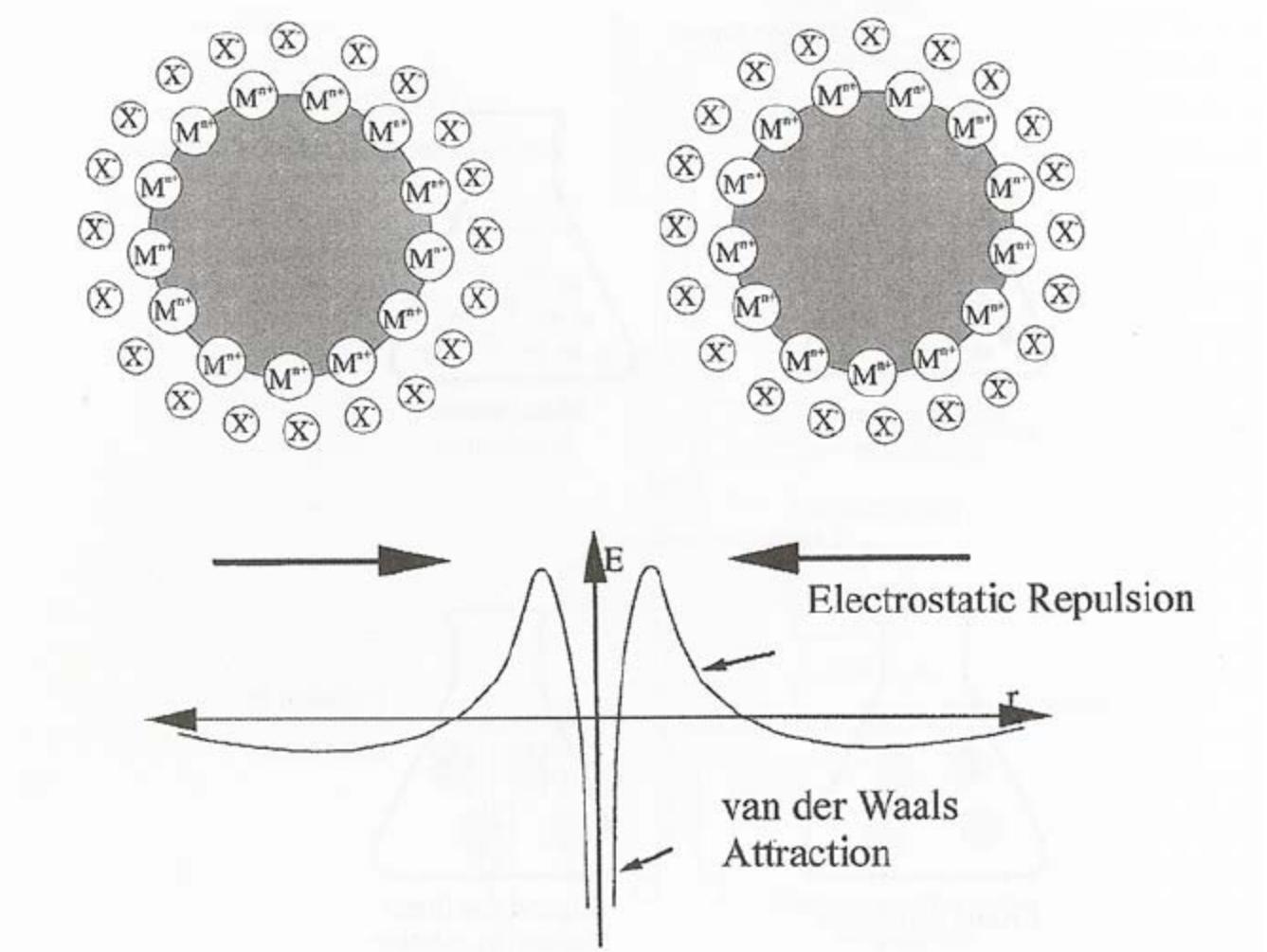

FIGURE 2.24 Electrostatic stabilization of metal colloids. Van der Waals attraction and electrostatic repulsion compete with each other.[27]

Net interaction energy governs stability

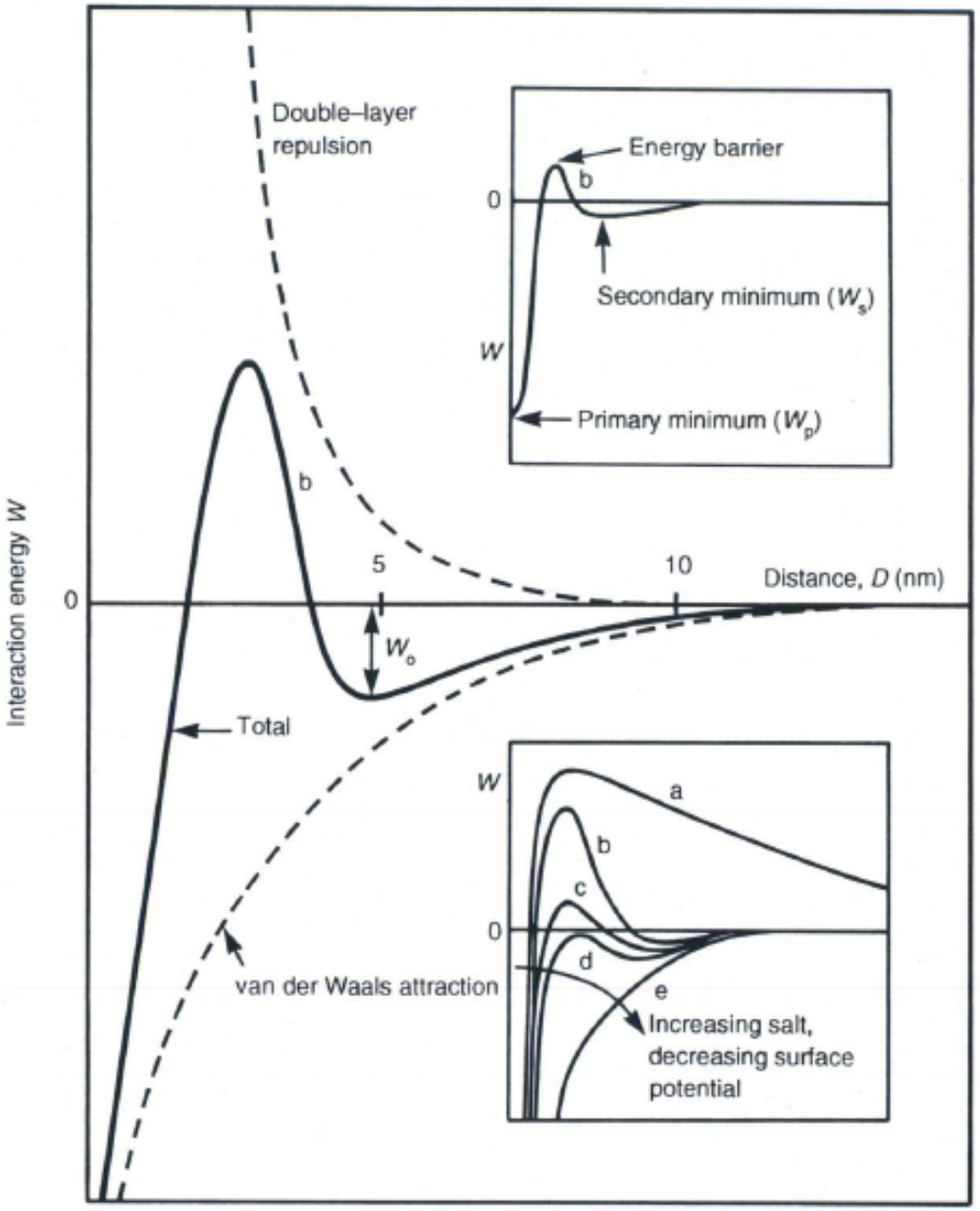

Fig. 12.12. Schematic energy versus distance profiles of DLVO interaction. (a) Surfaces repel strongly; small colloidal particles remain 'stable'. (b) Surfaces come into stable equilibrium at secondary minimum if it is deep enough; colloids remain 'kinetically' stable. (c) Surfaces come into secondary minimum; colloids coagulate slowly. (d) The 'critical coagulation concentration'. Surfaces may remain in secondary minimum or adhere; colloids coagulate rapidly. (e) Surfaces and colloids coalesce rapidly.

Israelachvili.

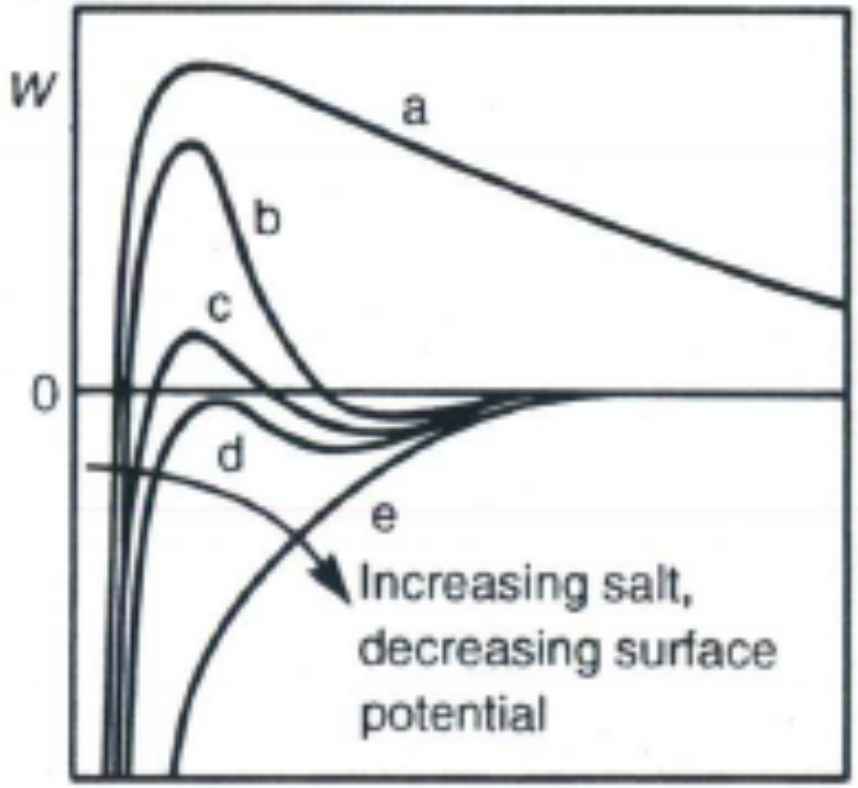

a) Strong long-range repulsion, fully dispersed
   - highly-charged surface in dilute electrolyte; long Debye length

b) Kinetically stable at secondary minimum or fully dispersed
   - higher electrolyte concentration than (a)

c) Slow aggregation
   - low surface charge density

d) Rapid coagulation

e) Effectively no repulsion

Israelachvili.

Example: interaction between a pair of Au particles

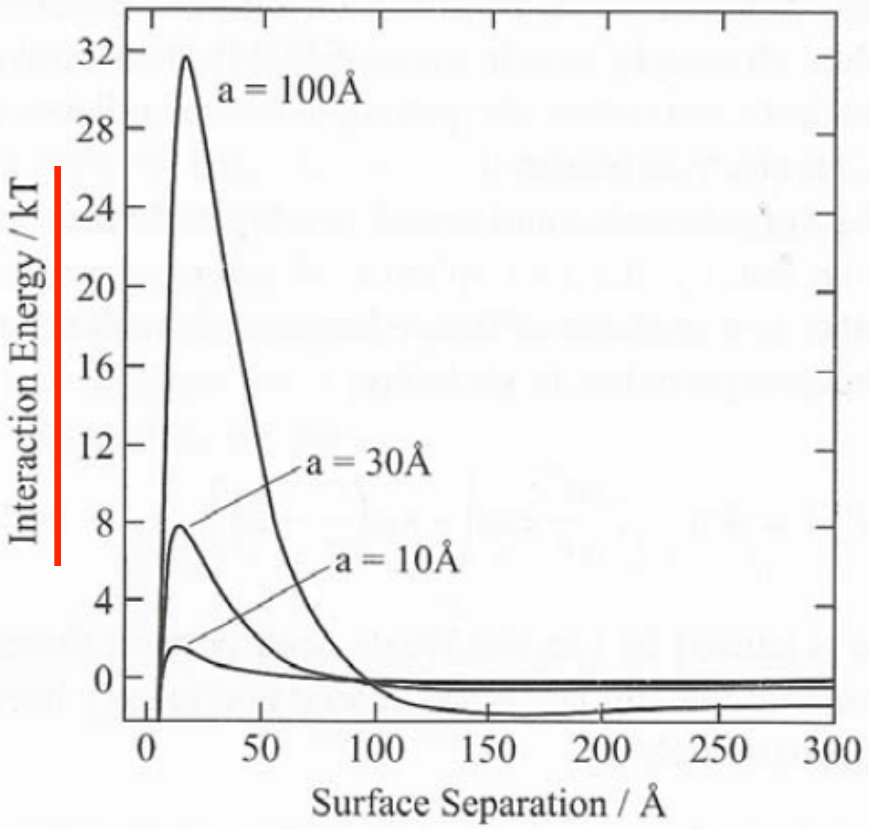

FIGURE 5.4 Plot of the interaction energy between two spherical gold particles in aqueous solution as a function of the particle separation, for several particle radii. Hamaker constant $= 25 \times 10^{-20}$ J, $I = 1$ mM, $\psi_0 = 0.10$ V, $a = 1.0$ nm, 3.0 nm, and 10.0 nm, Debye length = 10 nm. Note that the secondary minimum is negligible for nanoparticles, but becomes important above 10 nm.

Mulvaney.

Example: interaction between a pair of Au particles

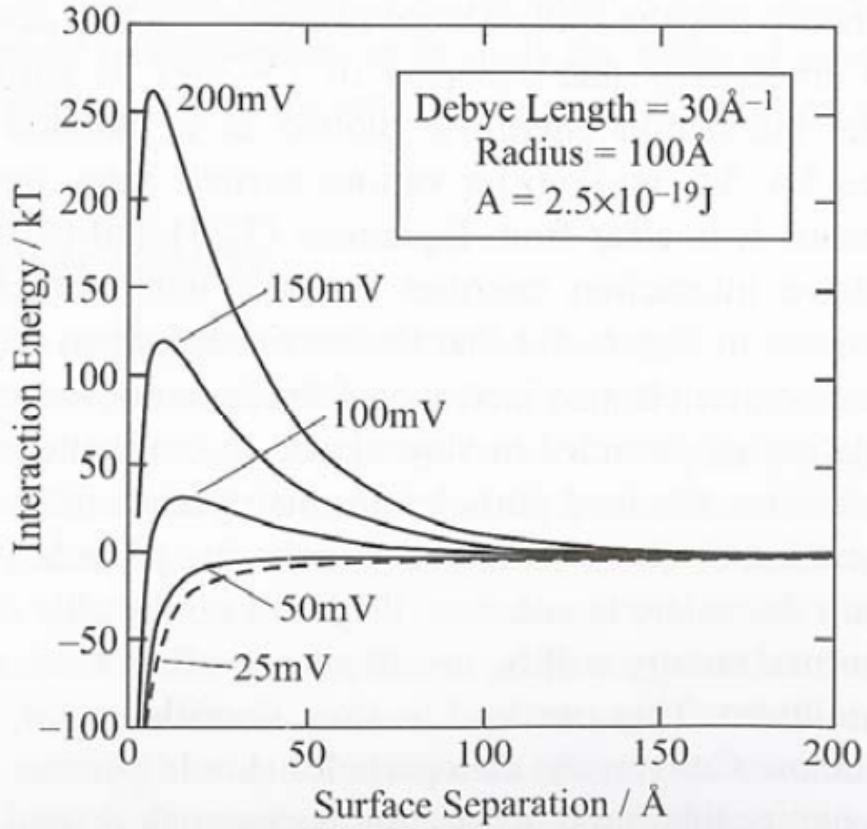

FIGURE 5.5 Plot of the interaction energy between two spherical gold particles in aqueous solution as a function of the particle separation for several surface potentials. Hamaker constant $= 25 \times 10^{-20}$ J, $I = 10$ mM, $a = 10$ nm, Debye length $= 3$ nm. Note that a zeta potential, $|\zeta| > 50$ mV, is necessary for colloid stability because of the high Hamaker constant.

Diffuse layer and Stern layer

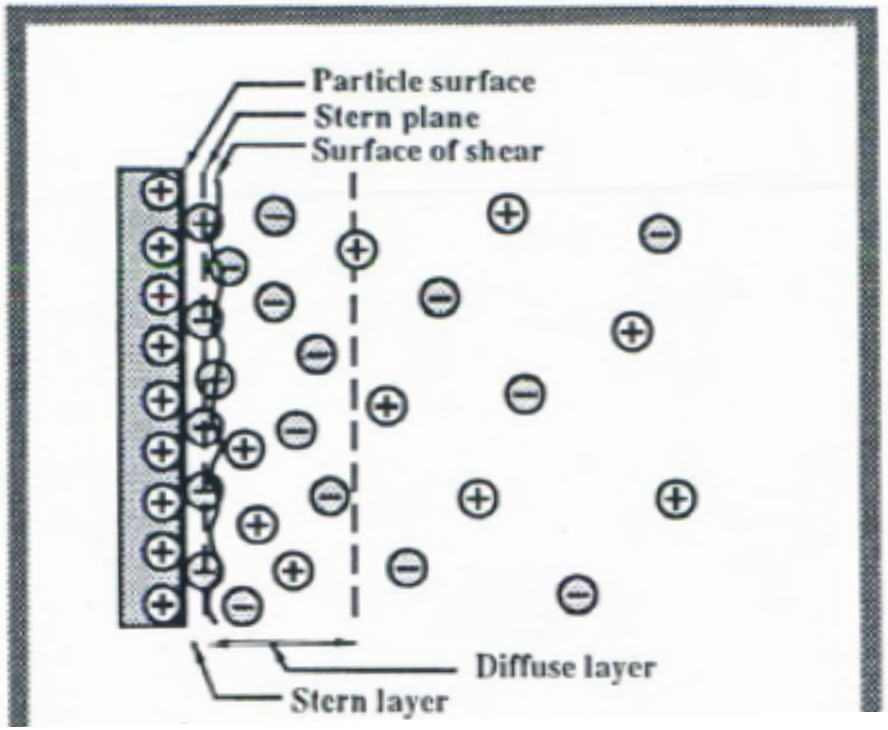

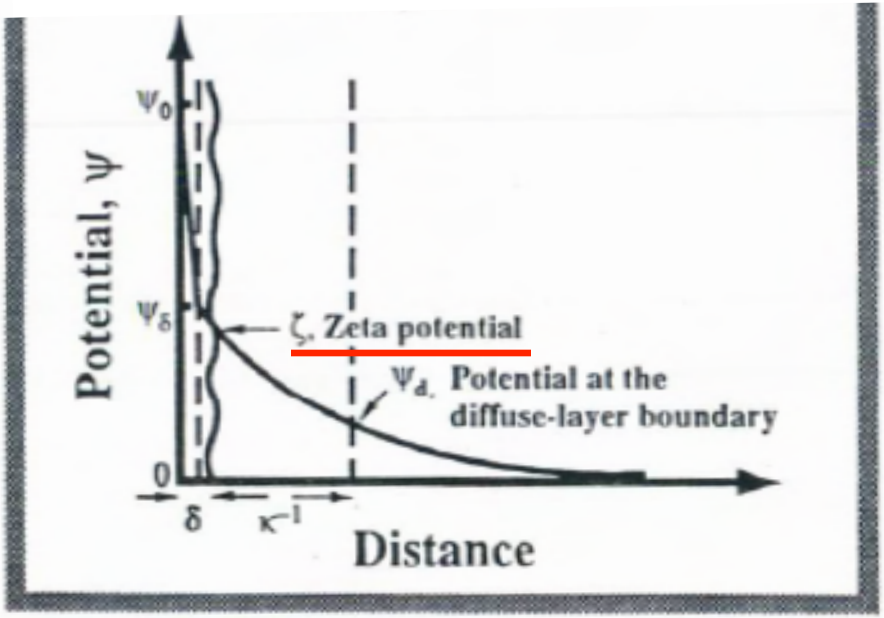

FIG. 11.9 Schematic illustration of the variation of potential the presence of a Stern layer. See Chapter 12 for discussion of s

- Zeta potential is typically measured
- Think about slip..

Hiemenz and Rajagopalan.

Overlapping double layers in a nanogap

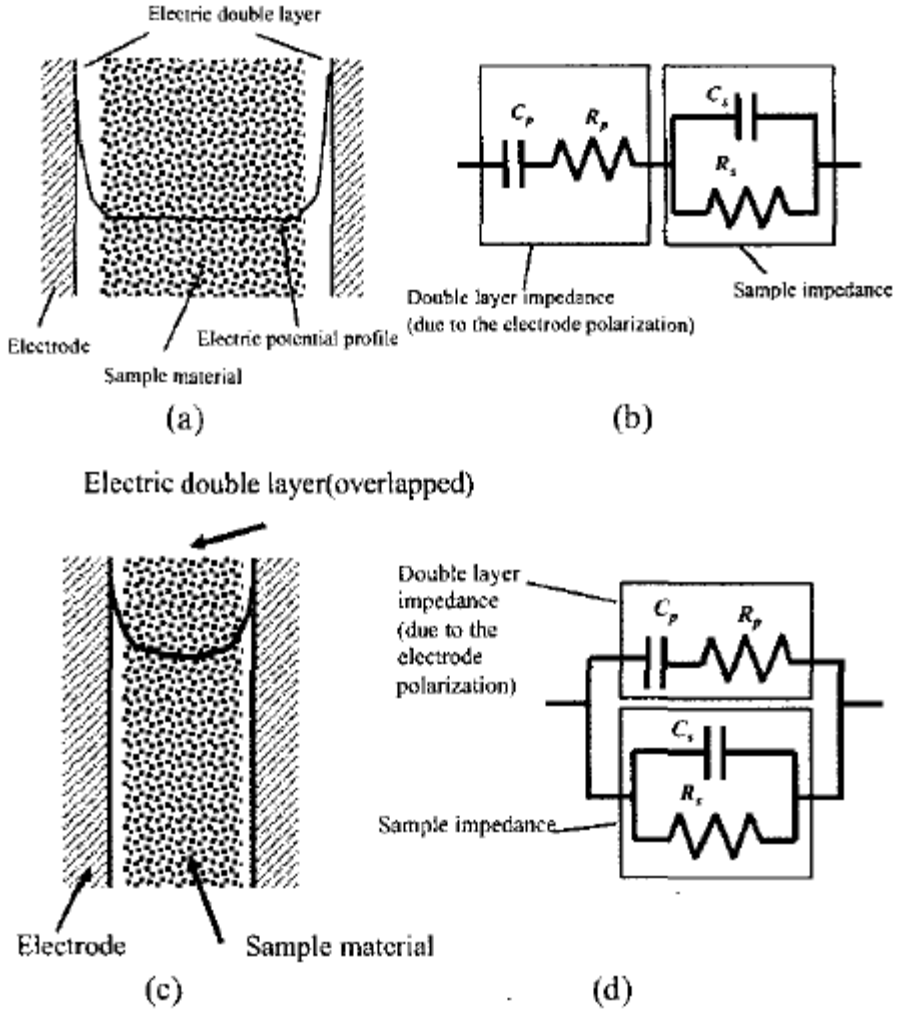

Figure 1: Schematic diagram and equivalent circuits of conventional electrode polarization (a) & (b) and nanogap electrodes (c) & (d).

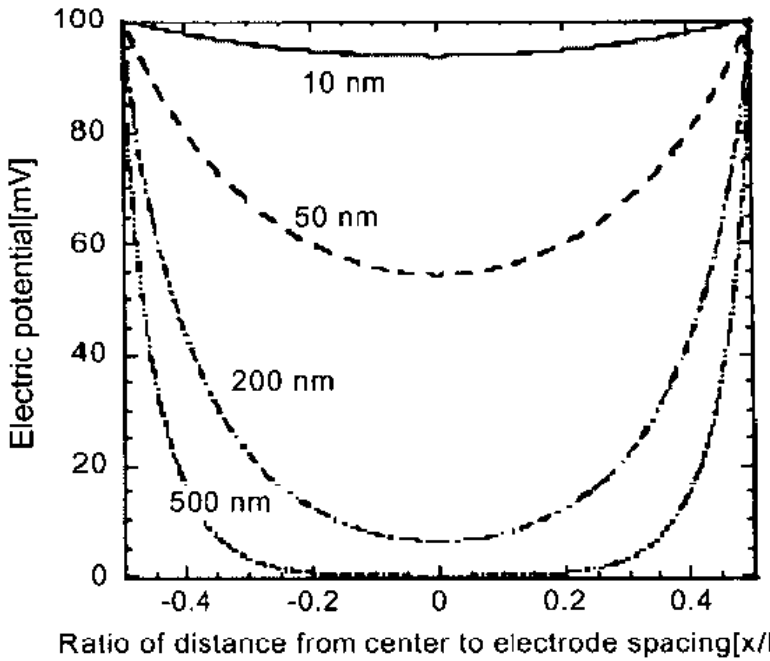

Figure 5: Electric potential between two electrodes for various channel width; the concentration of solution is 0.1mM of 1:1 electrolyte.

Oh et al., IEEE MEMS 03.

Nanofluidic transistors

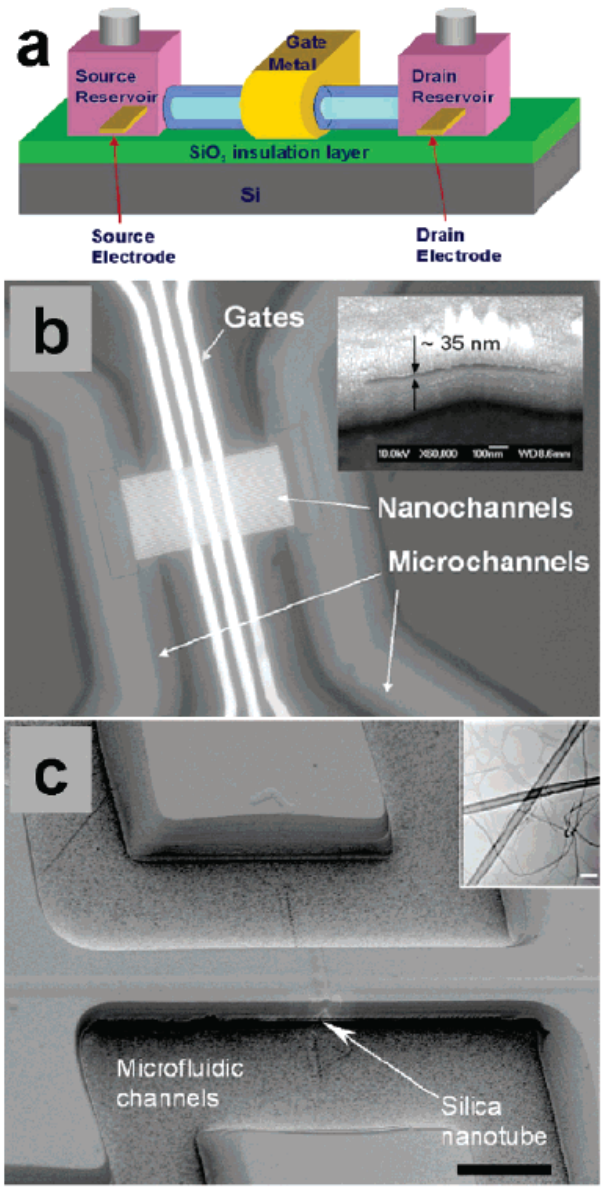

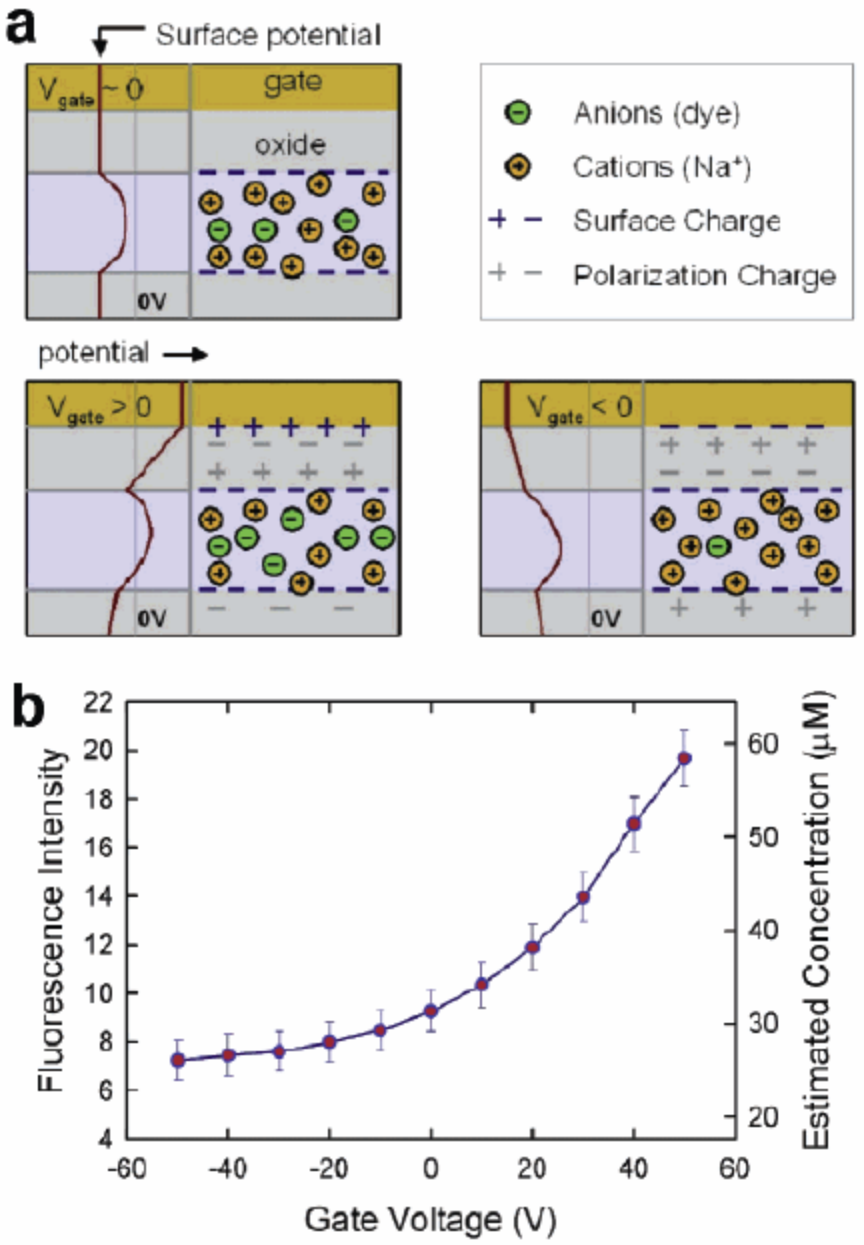

Karnik et al., Nano Letters 5(5):943-948, 2005.

Electrophoresis: placing particles in gaps

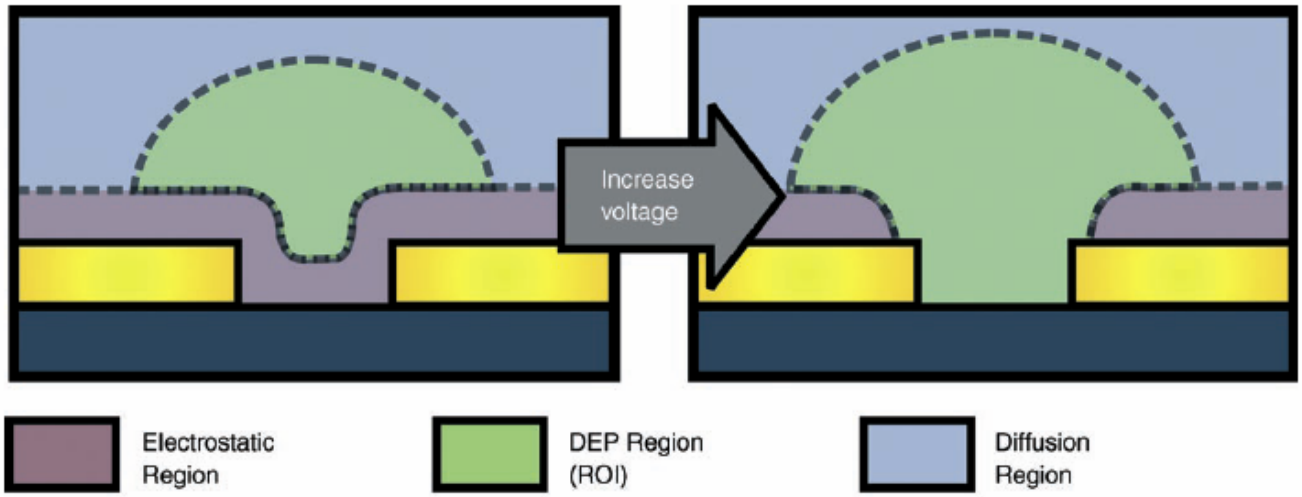

Figure 7. Schematic image showing regions where different forces dominate during DEP assembly of nanoparticles into nanogaps at voltages lower (left) and higher (right) than the threshold voltage.

- Motion is diffusive (Brownian) far from gap
- Substrate-particle repulsion dominates at low V
- "Spherical" DEP region grows and dominates at high V
- EP-induced oscillation only important at low frequencies

Barsotti et al., Small 3(3):488, 2007.

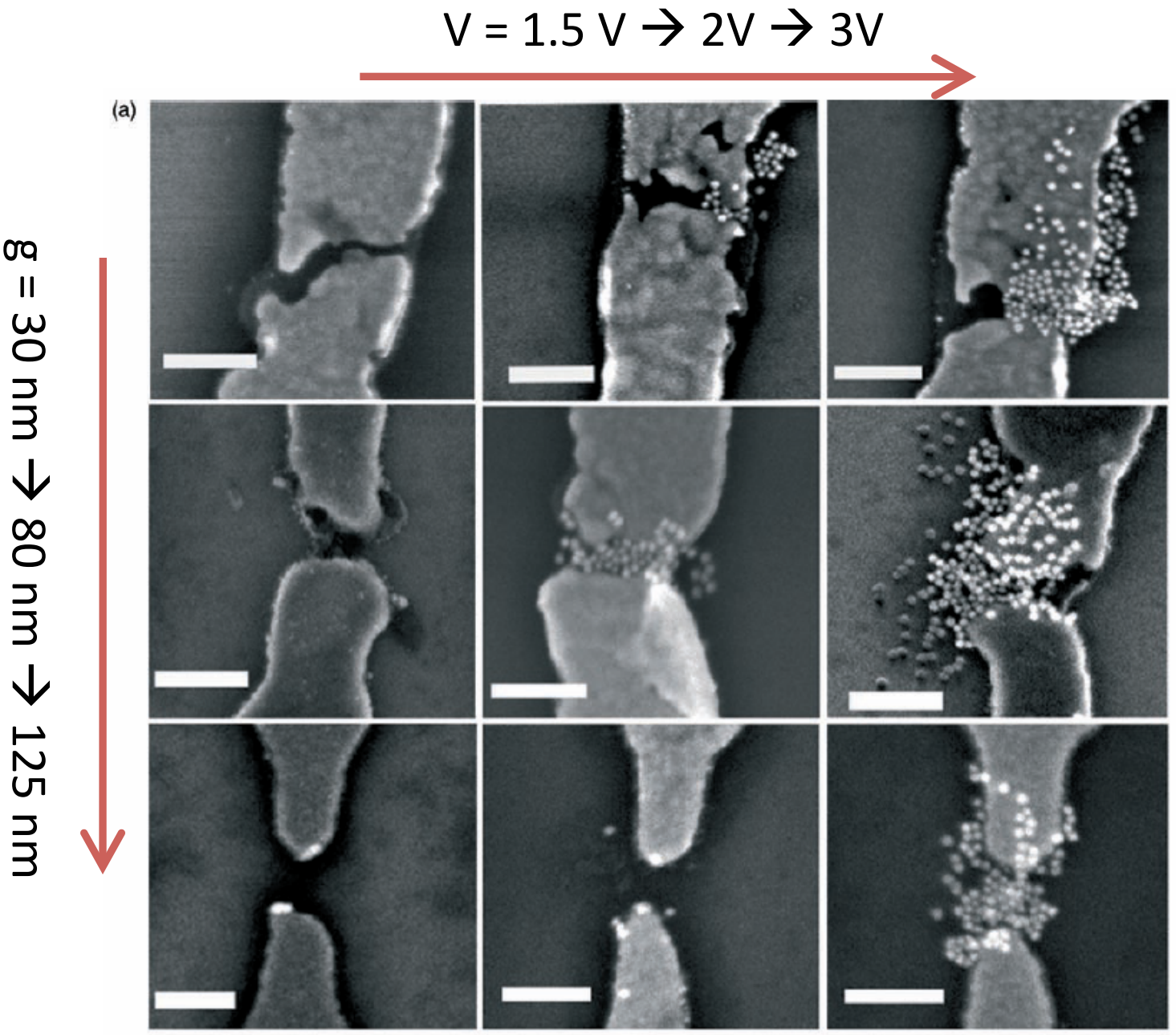

Barsotti et al., Small 3(3):488, 2007.

Dielectrophoresis for positioning CNTs

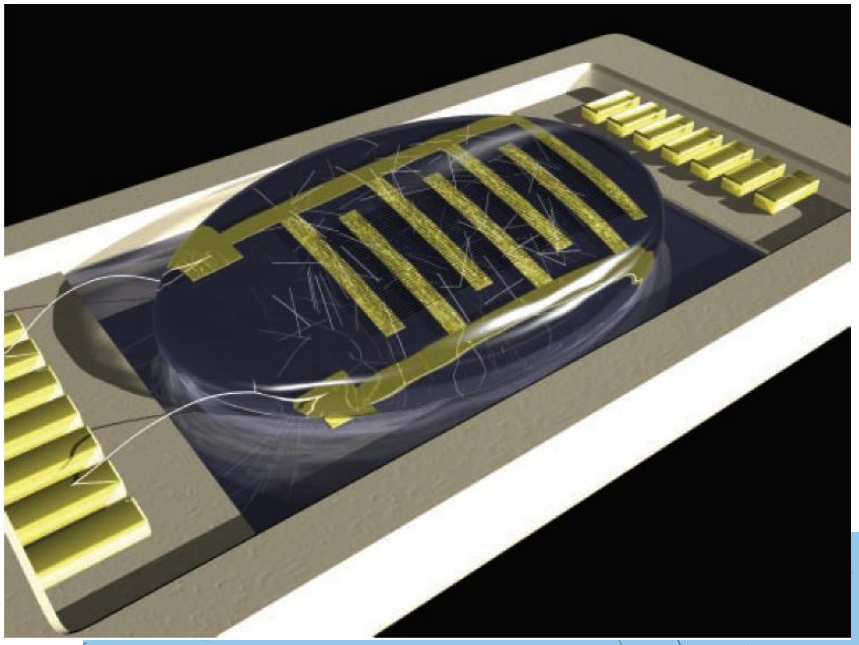

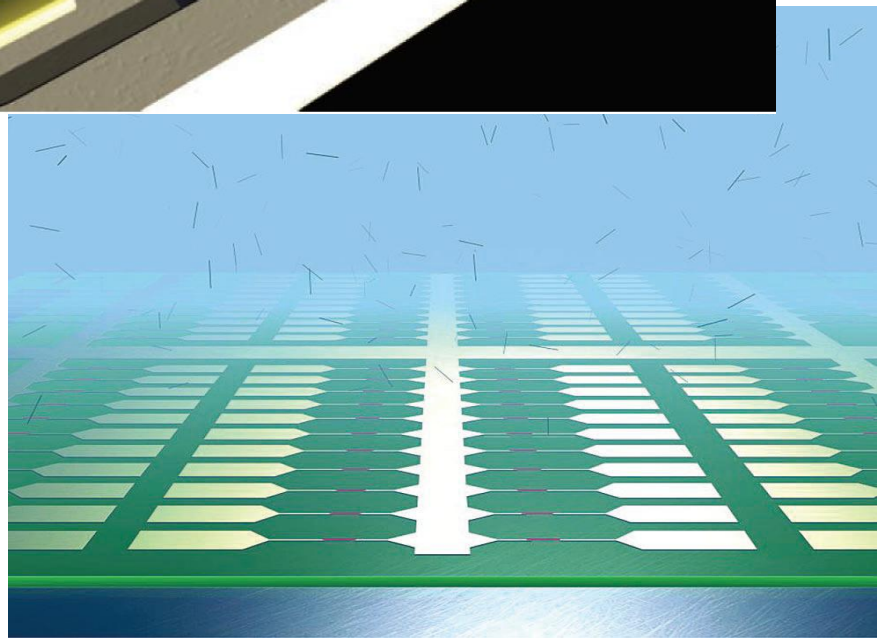

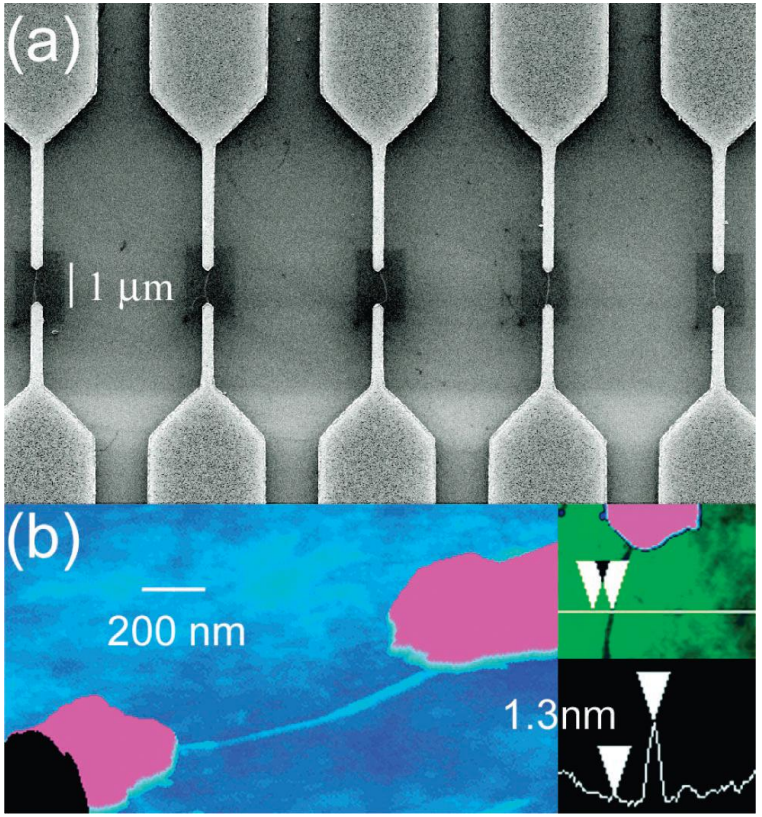

Vijayaraghavan et al., *Nano Lett*, V.7 No. 6, 1556-1560, 2007.

Electric field-directed growth of CNTs

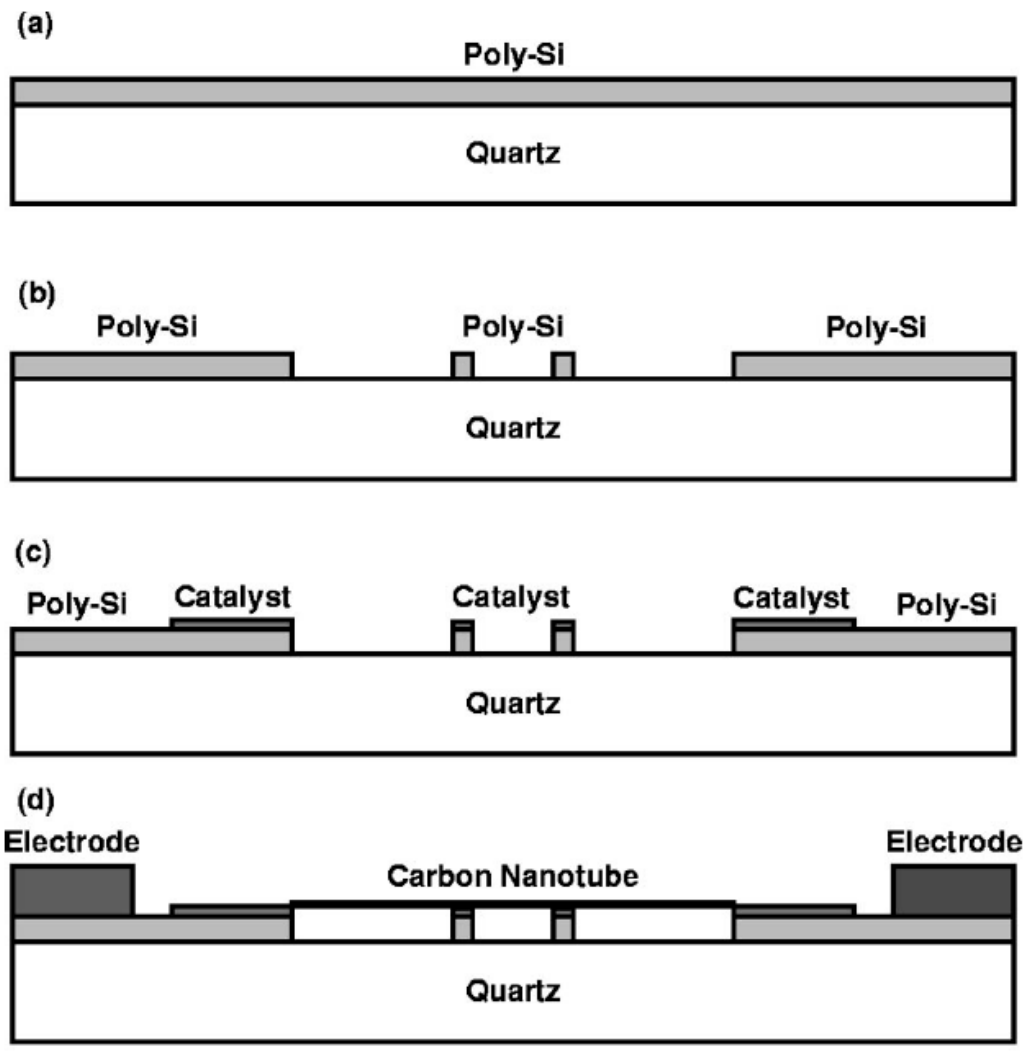

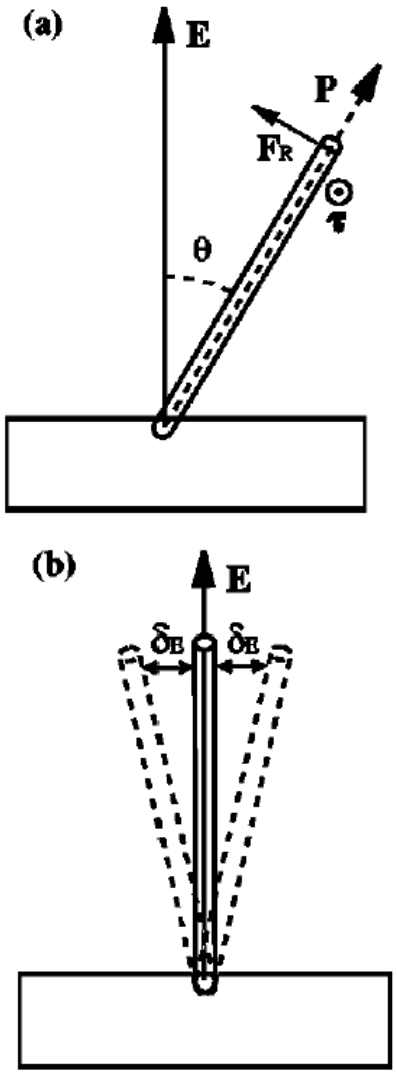

→ Alignment force vs. thermal vibration

Zhang et al., Applied Physics Letters 79, 2001

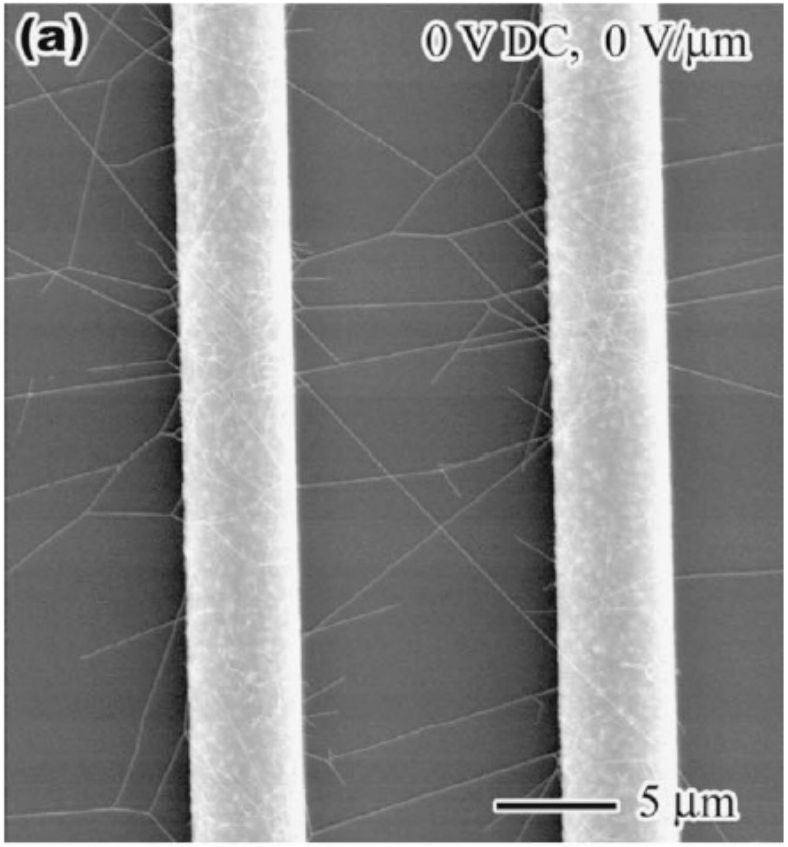

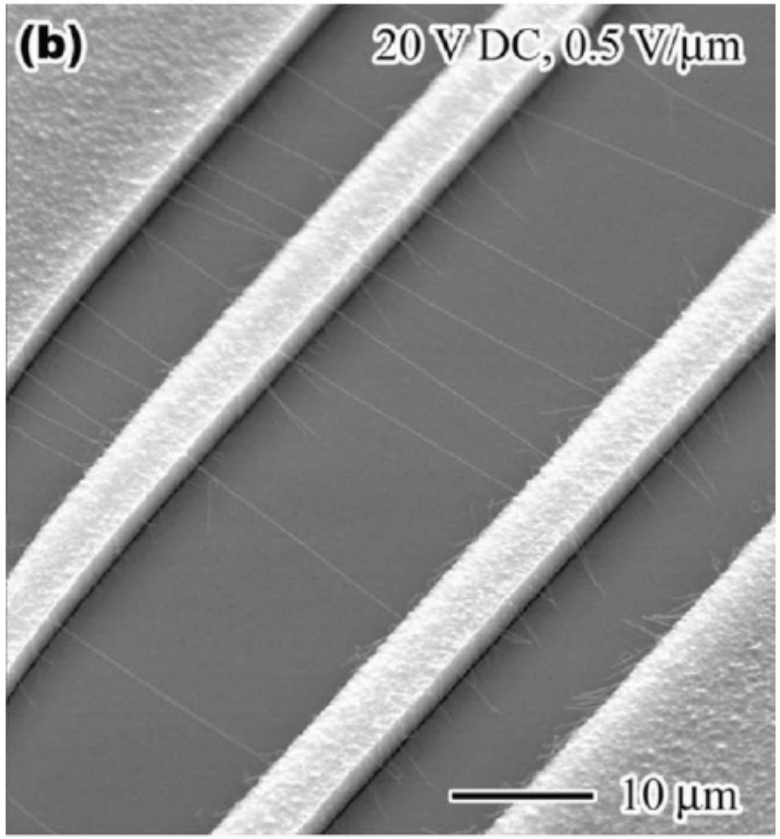

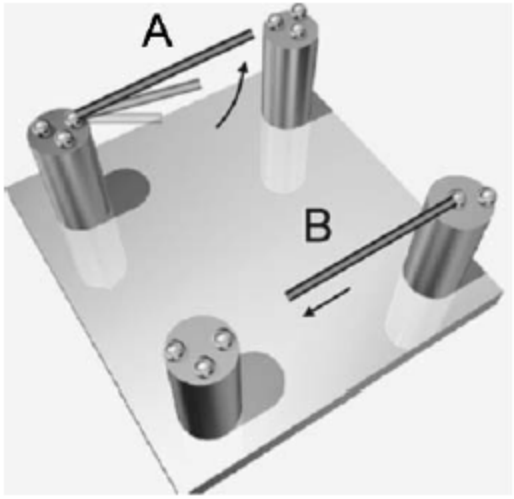

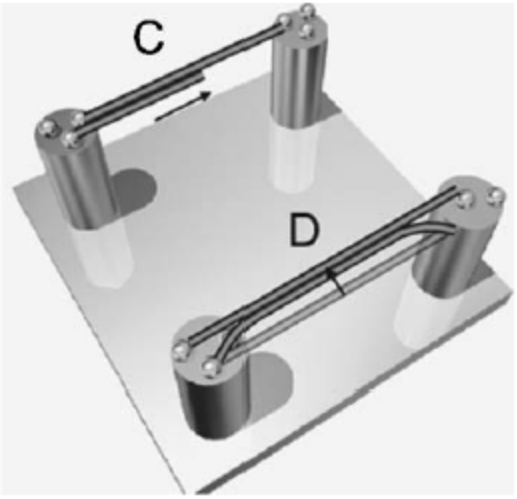

Zhang et al *Appl Phys Lett* 79, 2001
Homma et al *Appl Phys Lett* 88, 2006